# Comparison of the effectiveness of UV, UV/VUV photolysis, ozonation, and ozone/UV processes for the removal of sulfonamide antibiotics

Luca Farkas [a], Ilaria Monzini [b], Erzsébet Takács [c], László Wojnárovits [c], Mónika Vörös [d], Csaba Vágvölgyi [d], Csaba Janáky [e], Tünde Alapi [a,*]

[a] *University of Szeged, Institute of Chemistry, Department of Inorganic, Organic and Analytical Chemistry, Dóm tér 7., H-6720 Szeged, Hungary*
[b] *University of Padova, Department of Agronomy, Food, Natural resources, Animals and Environment, Via 8 Febbraio, 2–35122 Padova, Italy*
[c] *Radiation Chemistry Department, Institute for Energy Security and Environmental Safety, Centre for Energy Research, Konkoly-Thege Miklós út 29–33, H-1121 Budapest, Hungary*
[d] *University of Szeged, Institute of Biology, Department of Microbiology, Közép Fasor 52., H-6726 Szeged, Hungary*
[e] *University of Szeged, Institute of Chemistry, Department of Physical Chemistry and Material Sciences, Rerrich Béla sq. 1, H-6720 Szeged, Hungary*

## ARTICLE INFO

## ABSTRACT

UV (254 nm) and UV/VUV (254/185 nm) photolysis, ozonation, and $O_3$/UV combination were investigated and compared for the transformation of two sulfonamide (SAs) antibiotics, sulfamethazine (SMT) and sulfamethoxypyridazine (SMP). Change in toxicity, the effect of bacteria growth inhibition of the treated solutions, and the cost-efficiency of the methods were studied. In UV/VUV radiated solutions, the formation of $^{\bullet}OH$ results in the doubled transformation rate. The relative contribution of various ROS ($^{\bullet}OH$, $^1O_2$, $O_2^{\bullet-}$) to the transformations were also investigated in the case of UV and UV/VUV photolysis. Both SAs can be eliminated ten times faster during ozonation than UV photolysis; but conversion via ozonation is associated with the formation of products with low reactivity to ozone and has biological effects. The $O_3$/UV process did not enhance the transformation rate but positively affected mineralization and significantly decreased the ecotoxicity of the treated solutions. Ozonation was cost-effective, but $O_3$/UV is a much safer technology to minimize environmental impacts because it effectively reduces the ecotoxicity and the bacterial growth inhibition effect of the treated solution. The observed differences between SMT and SMP are primarily related to the transformation of the N-containing rings. Our results showed a correlation between the reactivity of the N-containing groups of SAs, the rate of mineralization, and the change in ecotoxicity and antibacterial effect and emphasized the need for toxicological characterization of the treated samples. The removal of parent compounds is not sufficient to avoid the release of toxic substances into the environment.

## 1. Introduction

Antimicrobial agents have been essential for treating human and animal diseases since the 1900s. However, the amount of antibiotics consumed for human disease treatment decreased from 2009 to 2018 [21]. However, total antibiotic consumption has increased significantly in recent years due to industrial-scale animal husbandry [16,28,55,75]. Furthermore, there is increasing interest in the contribution of hospital wastewater to the emerging antimicrobial resistance crisis in the environment [72]. As a result, a large amount of drug residues are discharged into wastewater and reach surface waters [8,65], ground waters [31,107], and are detected even in tap waters [23]. In recent years, the world has faced the COVID-19 pandemic. Although COVID-19 is a viral disease, infections often progress to bacterial infections requiring antibiotics. This way, the epidemic increased the global use of antibiotics and their concentration in wastewater [64,79].

The increase in antibiotic-resistant bacterial strains is a dangerous consequence of antibiotics in the environment and causes a global problem [54,65]. The European Antimicrobial Resistance Surveillance Network [21] estimates that more than 670,000 infections are caused by antibiotic-resistant bacterial strains in the European Union annually, generating approximately 33,000 deaths [21]. Sulfonamides are widely used antibiotics in veterinary medicine, accounting for 11% of total antibiotic sales [85]. Despite the decline in antibiotic use in the EU over

the last decade, sulfonamide consumption increased between 2009 and 2016 [21]. The extensive use is due to their broad spectrum against most Gram-positive organisms [15,20]. In addition to their multifaceted antibacterial, antifungal, and antiparasitic activity, sulfonamides and their derivatives show antiviral activity, and some of them have been tested as SARS-CoV-2 M[pro] inhibitors [5].

Sulfonamides are poorly absorbed in the body of animals, and a significant portion is excreted in urine and feces and enters the soil through organic fertilizers [86]. Due to their relatively high solubility in water [35,83] and mobility in soils [26], large amounts of drug residues penetrate the deep layer of the soil and pollute the groundwater [25]. They are detected worldwide in surface waters [71,103], and their concentration changes from $\mu g\ L^{-1}$ to mg $L^{-1}$.

Complete elimination of sulfonamides is difficult via conventional biological water treatment methods [90] partly because of the significantly reduced microbial diversity of the sludge culture [48,49]. Several publications deal with the photolysis of sulfonamides in various matrices using visible or UV light sources. Transformation can occur through direct or indirect photolysis; the latter involves (self-)photosensitization [18,59,105] and reactions with reactive oxygen-containing species (ROS), such as singlet oxygen ($^1O_2$) hydroperoxyl radical and superoxide radical ion ($HO_2^\bullet/O_2^{\bullet-}$) and even $^\bullet OH$ [11,37]. Direct UV photolysis generally results in $SO_2$ extrusion [18,50], while $^1O_2$ oxidation occurs in the amino moiety [37], and reaction with $^\bullet OH$ results in hydroxylation [51,58]. Primary products often preserve the basic structure of the parent compound, so products with ecotoxicity and antimicrobial effects are formed [93,101,105]. For sulfonamides, ozonation is adequate for their removal [40,41,56,60,106]. Radical-based methods are generally more effective for transforming and mineralizing organic substances than UV photolysis or ozonation. The combination of AOPs (UV/VUV [58], UV/TiO$_2$ [1,67,68], UV/Cl$_2$ [98], UV/S$_2$O$_8^{2-}$ [33], UV/H$_2$O$_2$ [108], UV/O$_3$, O$_3$/S$_2$O$_8^{2-}$ [46]) can further enhance efficacy.

Although several AOPs have been studied for antibiotic degradation [2], the ecotoxicity and antibacterial effect of the products remains questionable. The impact of acute toxicity of sulfamethoxazole and sulfathiazole for *Vibrio fischeri* increased [80,81], while that of sulfamethazine for *P. subcapitata* did not change during radiolytic treatment [52]. The 254 nm UV photolysis of sulfadiazine, sulfamethazine, sulfamethoxazole, and sulfathiazole was studied by Voight et al. [93]. The quantitative structure-activity relationship (QSAR) model and the determination of the minimal inhibitory concentration (MIC) against *Bacillus subtilis* and *Pseudomonas fluorescens* were used to assess the environmental hazard of the photoproducts. The QSAR model did not predict toxic intermediates, although the MIC value of the products was higher by factors 2.5 to 5 than the initial sulfonamides.

This work compares various supplementary water treatment methods to eliminate sulfonamide antibiotics, sulfamethazine, and sulfamethoxypyridazine. The UV photolysis (254 nm), UV/VUV photolysis (254/185 nm), ozonation, and O$_3$/UV (254 nm) processes are investigated and compared from various perspectives. The low-pressure mercury vapor lamp is a frequently used UV light source for water disinfection, which emits 254 nm UV and 185 nm VUV light. UV light is generally used for disinfection, while VUV photolysis efficiently decomposes hazardous organic substances [57,58,99,100,102]. Ozonation is a widely used method for pretreatment of wastewater, disinfection of treated waters, and selective oxidation of trace pollutants; its effectiveness is usually increased by 254 nm UV light. All investigated methods are used on an industrial scale [6,29,38], so it is justified to investigate and compare their effectiveness in removing sulfonamides from water. The investigation of the ecotoxicity and bacterial growth inhibition effect of the treated samples and the electrical energy requirement of the methods were also important aspects.

## 2. Materials and methods

### 2.1. Materials

Analytical standards for sulfamethazine (SMT) and sulfamethoxypyridazine (SMP) (99%) were purchased from Sigma-Aldrich®. HPLC grade methanol (MeOH), tert-butanol (t-BuOH) (>99%), formic acid (99–100%), NaCl (99%), NaOH (99%), and HCl solution were purchased from VWR. Triethylenediamine (TEDA) (>99%), Furfuryl alcohol (FFA) (>98%) and L-histidine (L-his) (>99%), and 1,4-hydroquionone (1,4-Dihydroxybenzene, HQ) (>99%) were purchased from Sigma-Aldrich®. Ultrapure water was produced by a Milli-Q Integral Water Purification System (MerckMillipore). The O$_2$ (99.5%), N$_2$ (99.995%), and air were provided by Messer Hungarogáz Kft.

### 2.2. Light sources and experimental apparatus

Two low-pressure mercury vapor (LP) lamps (GCL307T5L/CELL and GCL307T5VH/CELL, 227 mm arc length, both produced by LightTech) were used for UV (254 nm) and UV/VUV (254 nm/185 nm) irradiation. Both lamps had the same technical parameters (electric power 15 W, UVC-flux power 4.3 W; diameter: 20.5 mm, length: 307 mm). The envelope of the UV lamp was made of commercial quartz, whereas that of the UV/VUV lamp was made of synthetic quartz to transmit 185 nm photons. The flux of 254 nm photons of both lamps (UV and UV/VUV) was determined by ferrioxalate actinometry [45] and was found to be the same ($5.3(\pm 0.3)\times 10^{-6}$ mol$_{photon}$ s$^{-1}$). The flux of the 185 nm VUV photons ($3.86(\pm 0.11)\times 10^{-7}$ mol$_{photon}$ s$^{-1}$) was determined by methanol actinometry [70] and found to be one order of magnitude lower than that of UV photons.

Photochemical experiments were carried out in a 500 cm$^3$ cylindrical glass reactor (Fig. S1) having a 60 mm inner diameter and 300 mm height. The thickness of the irradiated water layer was 20 mm, sufficient for the complete absorption of 185 nm photons [3]. The reactor was thermostated at room temperature (25 $\pm$ 1 °C). A glass filter disc was used at the bottom of the reactor to disperse the gas (oxygen, air, nitrogen, or ozone/oxygen mixture) in the total volume of the treated aqueous solution. The dissolved O$_2$ concentration was 40 mg dm$^{-3}$ in the case of O$_2$ saturated solutions, while in the case of N$_2$ bubbling, the O$_2$ concentration was less than 0.6 mg dm$^{-3}$. In the ozonation experiments, O$_3$ gas was supplied by an Ozomatic Modular 4HC type ozonator, using O$_2$ (500 cm$^3$ min$^{-1}$) as the feeding gas. Treatment started by turning on the light source or the ozonator.

### 2.3. Analytical methods

Spectrophotometric measurements were made with an Agilent 8423 UV-Vis spectrophotometer using a quartz cuvette. The concentration of O$_3$ ranged from 1.0 to 4.2 × 10$^{-4}$ M in the gas flow. The O$_3$ concentration in the gas phase was determined at 254 nm ($\varepsilon_{254\ nm}$ = 2950 M$^{-1}$ cm$^{-1}$ [104]) according to the Lambert-Beer law in a flow-through 1.00 cm gas cuvette.

Fluorescence spectroscopy (Hitachi F4500) was applied to determine the fluorescence emission spectrum of SMT and SMP. The wavelength of excitation was 254 nm.

The concentration of SMT and SMP was measured using an Agilent 1100 HPLC coupled with a diode array detector (DAD). The column (Lichrospher 100, RP-18; 5 µm) was thermostated at 25 °C, and the flow rate of the eluent (methanol:water (0.1% formic acid) = 35:65 (v/v) mixture in the case of SMT and methanol: water (0.1% formic acid) = 30:70 (v/v) mixture in the case of SMP) was 1.0 cm$^3$ min$^{-1}$. The detection was performed at 266 nm. Under these conditions, SMT and SMP were eluted at 8.9 and 6.5 min, respectively.

The intermediate products of SMT and SMP were identified using an Agilent LC/MSD VL mass spectrometer coupled to the HPLC device. Solid phase extraction (SPE) was used as a sample pretreatment method.

After conditioning (1.0 cm$^3$ of water and 1.0 cm$^3$ of methanol), 50 cm$^3$ of the sample was loaded into the Phenomenex Stata-X 33 u cartridge. After washing (1.0 cm$^3$ of water) and drying (10 min), elution was performed using 2.0 cm$^3$ methanol. The MS system was operated in positive electrospray ionization (ESI) mode (3.5 kV capillary voltage, 300 °C drying gas temperature, and 70 V fragmentor voltage). In all cases, the separation occurred in the reverse phase, on a Lichrospher 100 column, RP-18 (5 μm), with a flow rate of 0.9 cm$^3$ min$^{-1}$. For the SMT separation, gradient elution was used: the mobile phase was a mixture of water containing 0.1% formic acid (A) and methanol (B). After 14 min of isocratic elution, the methanol content increased from 20% to 70% during 25 min. For SMP separation, isocratic elution was used (70% water containing 0.1% formic acid and 30% methanol).

Inorganic ions formation ($NH_4^+$, $NO_2^-$, $NO_3^-$, and $SO_4^{2-}$) was measured using ion chromatography (Shimadzu Prominence LC-20AD). Shodex 5 U-YS-50 column for cation detection (eluent contained 4.0 mM methanesulfonic acid and 2.5 mM phthalic acid) and Shodex NI-424 5 U for anion detection (eluent: 2.3 mM aminomethane solution). The flow rate of the mobile phase was 1.0 cm$^3$ min$^{-1}$.

The total organic carbon (TOC) content of the samples was determined using a Multi N/C 3100 analyzer (Analytik Jena) equipped with an NDIR detector. The concentration of $H_2O_2$ (0.015 - 6.00 mg dm$^{-3}$) was determined using a colorimetric test kit (Merck-Millipore), using a Spectroquant® Multy Vis-spectrophotometer.

### 2.4. Determination of the initial transformation rate and the quantum yield

The transformation of SMP and SMT was characterized by the initial rate of degradation ($r_0$ (M s$^{-1}$)), obtained from the linear regression fit to the concentration-time plot, generally up to 20% transformation. Some experiments were repeated three times to verify the reproducibility of the experimental results. Quantum yield ($\Phi_{254 \text{ nm}}$) of SMP or SMT photolysis at 254 nm was calculated as follows:

$$\Phi_{254 \text{ nm}} = r_0/[\varphi_0 \times (1 - 10^{-\varepsilon \times c0 \times l})]$$

where $r_0$ is the initial transformation rate determined in UV-irradiated solutions, at the initial concentration ($c_0$), $\varphi_0$ is the photon flux of 254 nm per volume unit (mol$_{photon}$ s$^{-1}$ dm$^{-3}$), $\varepsilon$ is the molar absorption coefficient determined at 254 nm, and l (cm) is the thickness of the irradiated layer of the aqueous solution (2.0 cm).

### 2.5. Ecotoxicity test

The ecotoxicity test based on bioluminescence measurements of the marine bacteria *Vibrio fisheri* (*V. fisheri*) (LCK480 test from Hach Lange) was used. The pH and NaCl concentration of each sample were adjusted to 6.5–8.0% and 2.0% w/v, respectively. The dissolved $O_3$ was eliminated from each sample by nitrogen bubbling, while $H_2O_2$ was eliminated by 0.20 mg dm$^{-3}$ catalase enzyme (Sigma Aldrich, 2000–5000-unit mg$^{-1}$). Inhibition of bioluminescence was measured using a Lumistox 300 (Hach Lange) luminometer after 15 min of incubation time. The control sample was Milli-Q water containing 2.0% w/v NaCl, while the standard (50 ± 10% inhibition) contained 7.5% w/v NaCl. In each case, two parallel measurements were made.

### 2.6. Antimicrobial susceptibility and bacterial growth inhibition tests

The antibiotics (1.0 ×10$^{-4}$ M) were dissolved in double distilled water and filtered by a 0.45 μM syringe filter (Millex-HV, Millipore)· $H_2O_2$ and dissolved $O_3$ were eliminated from samples taken during the oxidation processes. Gram-positive *Bacillus subtilis* SZMC 25449 and *Micrococcus luteus* SZMC 0264, and Gram-negative *Escherichia coli* SZMC 6271 (SZMC: Szeged Microbiological Collection) were used for the antimicrobial susceptibility tests. Mueller-Hinton (MH) liquid medium

(VWR) was utilized for bacterial cultivation. The strains were cultured overnight in MH liquid medium in an orbital shaker (KS 3000ic control, IKA; 120 rpm, 30 °C). The overnight bacterial cultures were diluted in 10 times concentrated Mueller-Hinton broth to 10$^5$ CFU/cm$^3$. The experiments were prepared at 96-well microtiter plates in 200 μl volume: 180 μl of antibiotic solution and 20 μl of 10 times concentrated MH broth with 10$^5$ CFU/cm$^3$ were measured in wells. The bacterial growth was quantified with a microplate reader (SPECTROstar Nano; BMG Labtech, Offenburg, Germany) every 30 min at 620 nm for 20 h. In each case, two parallel measurements were made.

### 2.7. Electrical Energy per Order (EEO) calculations

Electrical energy per order ($E_{EO}$) represents the amount of electrical energy required for the reduction of the target compound concentration in a unit volume (i.e., 1 m$^3$) by one order of magnitude [17]. In batch operation, the $E_{EO}$ values (kWh m$^{-3}$ order$^{-1}$) can be calculated using the equation:

$$E_{EO} = \frac{P \times t \times 1000}{V \times \lg(c_i/c_f)}$$

where $P$ is the rated power (kW) of the AOP system (electrical power of the light source and the ozone generator), $V$ is the volume (dm$^3$) of water, $t$ is the treatment time (h), $c_i$ and $c_f$ are the initial and final concentrations (M), respectively, of the compound investigated. Factor 1000 converts dm$^3$ to m$^3$.

## 3. Results and discussion

### 3.1. UV photolysis

The molar absorbance of the sulfonamides was determined at 254 nm; the values were 17,550 M$^{-1}$ cm$^{-1}$ for SMT (pH = 6.4), and 16,280 M$^{-1}$ cm$^{-1}$ for SMP (pH = 6.7), similar to the data reported previously [32,58]. In the case of UV photolysis, the degradation rate increased with the initial concentration up to 5.0 × 10$^{-5}$ M (Fig. 1.) due to the complete absorption of 254 nm photons. The apparent quantum yield of the UV-initiated transformation was 0.0066 for SMT, and a slightly lower value of 0.0060 was determined for SMP. The data in the relevant literature are contradictory: Baeza and Knappe determined a value of 0.0087 [9], while Li et al. determined 0.019 [58] for the photolysis of SMT. Nassar et al. Nassar et al., ($year$) [69] reported lower values: 0.0043 for SMT and 0.0051 for SMP. The different pH values of the treated solutions may partially cause the discrepancy in the data.

Protonation can affect the molar absorbance, the quantum yield of direct photolysis [22], and the reactivity towards reactive species [37]. In the range of pH 3 – 10, the change in the shape of the spectrum (Fig. S2) reflects the sulfonamide nitrogen protonation process (pK$_a^{SMT}$ = 7.0 and pK$_a^{SMP}$ = 7.3 ([76,89], Nassar, 2017)). However, the transformation rate of SMT increases slightly in the pH range of 4 – 9, while that of SMP is practically pH-independent (Fig. S2) in the case of UV photolysis. Further experiments were carried out without setting pH (pH$^{SMT}$ = 6.4; pH$^{SMP}$ = 6.7).

The absorption of a 254 nm photon results in a singlet excited state of the molecule, which can transform into a triplet excited state; generally, its further reactions induce the transformation of sulfonamides [18,50, 59,69,105]. The relaxation includes the bound breaking and formation of photoproducts (direct photolysis processes) or the radiation process. In contrast to SMP, the solution of SMT irradiated with 254 nm light fluoresces intensely (Fig. S3). Fluorescence confirmed that the singlet excited state of SMT can undergo an intersystem crossing into a triplet excited state, which plays a vital role in photosensitized processes. Thus, in addition to direct photolysis, the reaction with ROS, photosensitization, and even self-sensitization can co-occur with the direct photolysis
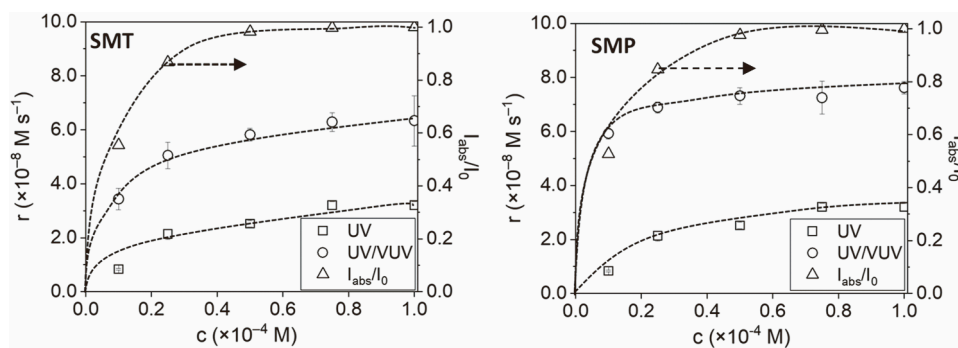
**Fig. 1.** The transformation rate of SMT and SMP in UV and UV/VUV irradiated solutions saturated with air (the second axis shows the absorbance at 254 nm versus the initial concentration).

in UV irradiated solutions of sulfonamides [11,37,105]. The relative contribution of $^{\bullet}OH$, $^1O_2$, and $O_2^{\bullet-}$ was investigated by the effect of various scavengers. An essential aspect of selection scavengers was avoiding competition for 254 nm photons with SMP and SMT (Fig S4).

The t-BuOH was used as a $^{\bullet}OH$ scavenger, while L-His, TEDA and FFA were used to investigate the role of $^1O_2$ [30,44,53,62,95] (Table S1-S3 and Fig. S5 and S6). The HQ reacts with $^{\bullet}OH$, $^1O_2$, and $O_2^{\bullet-}$ [4,77,91]; thus its effect is quite complex. Based on a careful evaluation of the
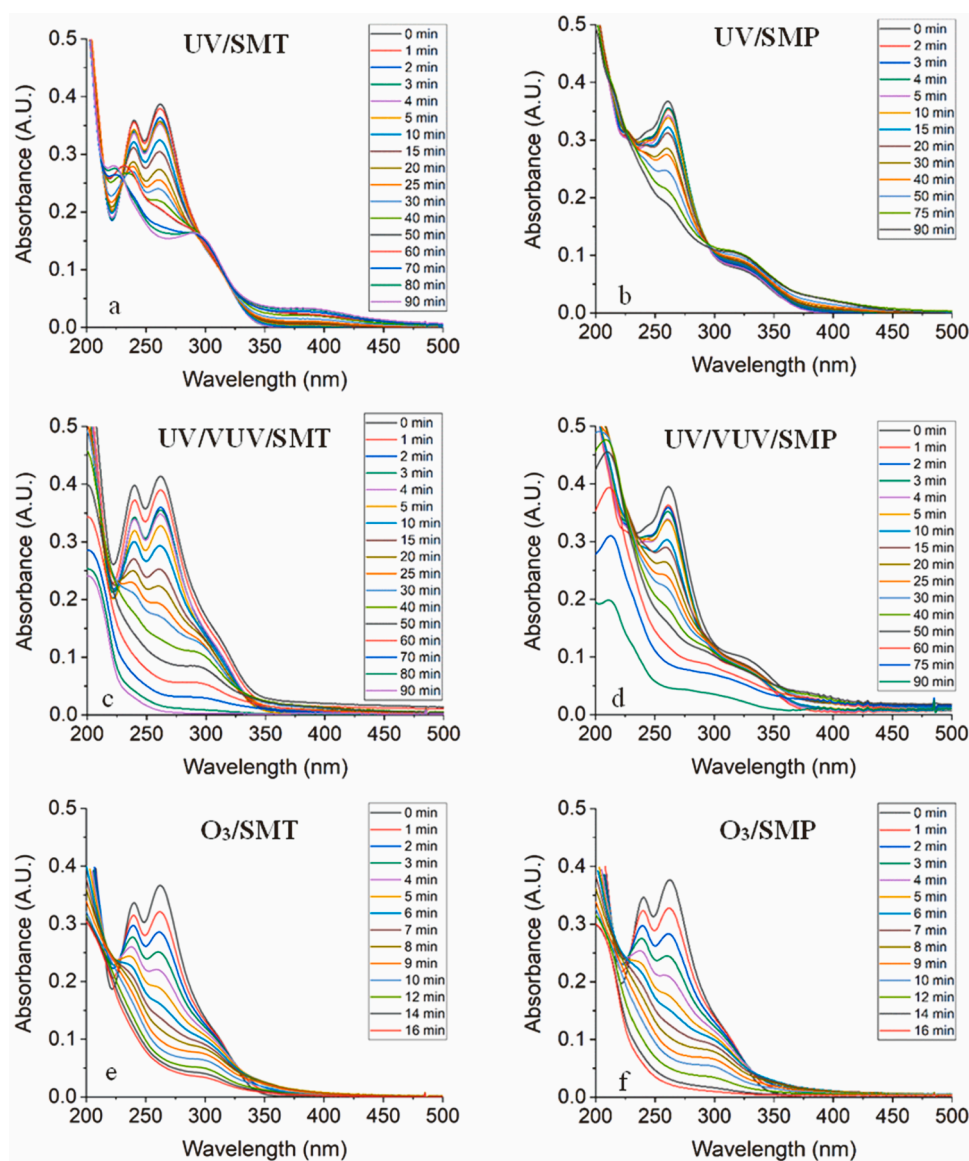


**Fig. 2. :** The UV-Vis absorption spectra of the treated SMT and SMP ($c_0 = 1.0 \times 10^{-4}$ M) solutions during UV (a and b), UV/VUV photolysis (c and d) in aerated solutions, and ozonation ($c(O_3) = 1.3 \times 10^{-4}$ M) (e and f).

effect of scavengers, the contribution of different ROS to the transformation can be determined. The contribution of •OH is less than 5% for SMT and 15% for SMP. The contribution of $^1O_2$ is no more than 10% for both SA, while $O_2^{\bullet-}$ has role (about 25%) only in the case of SMT transformation. Obviously, the contribution of various ROS in SMP transformation is more significant than in SMT transformation (Table S3 and Fig. S6). The experimental results (Fig S4-S6 and Table S1-S3) rand their detailed evaluation can be found in the Supplementary file.

The changes in the UV-Vis spectrum of the samples (Fig. 2) provide information on the processes that occur in the solution during treatment. Detailed spectral changes in all investigated solutions are shown in Figs. S7 and S8. The characteristic peak of the UV absorption spectrum, around 260 nm (263 nm for SMT and 261 nm for SMP), refers to the benzene ring, while the peak around 240 nm refers to the heterocyclic ring. Differences in the spectra can be observed because of the pyrimidine (SMT) and pyridazine (SMP) rings and their substituents.

In UV photolysis, the formation of new compounds occurs with absorption spectral shifts to smaller wavelengths, compared to the spectra of SMT or SMP (Fig. 2a and b). The decrease in absorbance around 260 and 240 nm, characteristic of the benzene and heterocyclic rings, was much slower than the decrease in the concentration of sulfonamides (Fig. S9). The absorbance change at these wavelengths slowed after the transformation of SMT and two isosbestic points appear at 231 and 290 nm (less characteristic) (Fig. 2a), suggesting the presence of two species having the same molar absorption coefficient at these wavelengths. A similar phenomenon was observed for SMP, where the isosbestic points were at 234 (less characteristic) and 290 nm (Fig. 2b). Based on product studies published in the literature, we assume; it is probably due to –(SO$_2$) extrusion.

Dissolved O$_2$ did not have significant affect the transformation rate (Fig. S10), but the spectrum changes slightly depending on that (Figs. S7 and S8). The manifestation of the isosbestic points and the absorbance change between 300 – 400 nm (increased only in the O$_2$-free solution of SMT (Fig. S7)) is affected by the presence of O$_2$, supporting that the
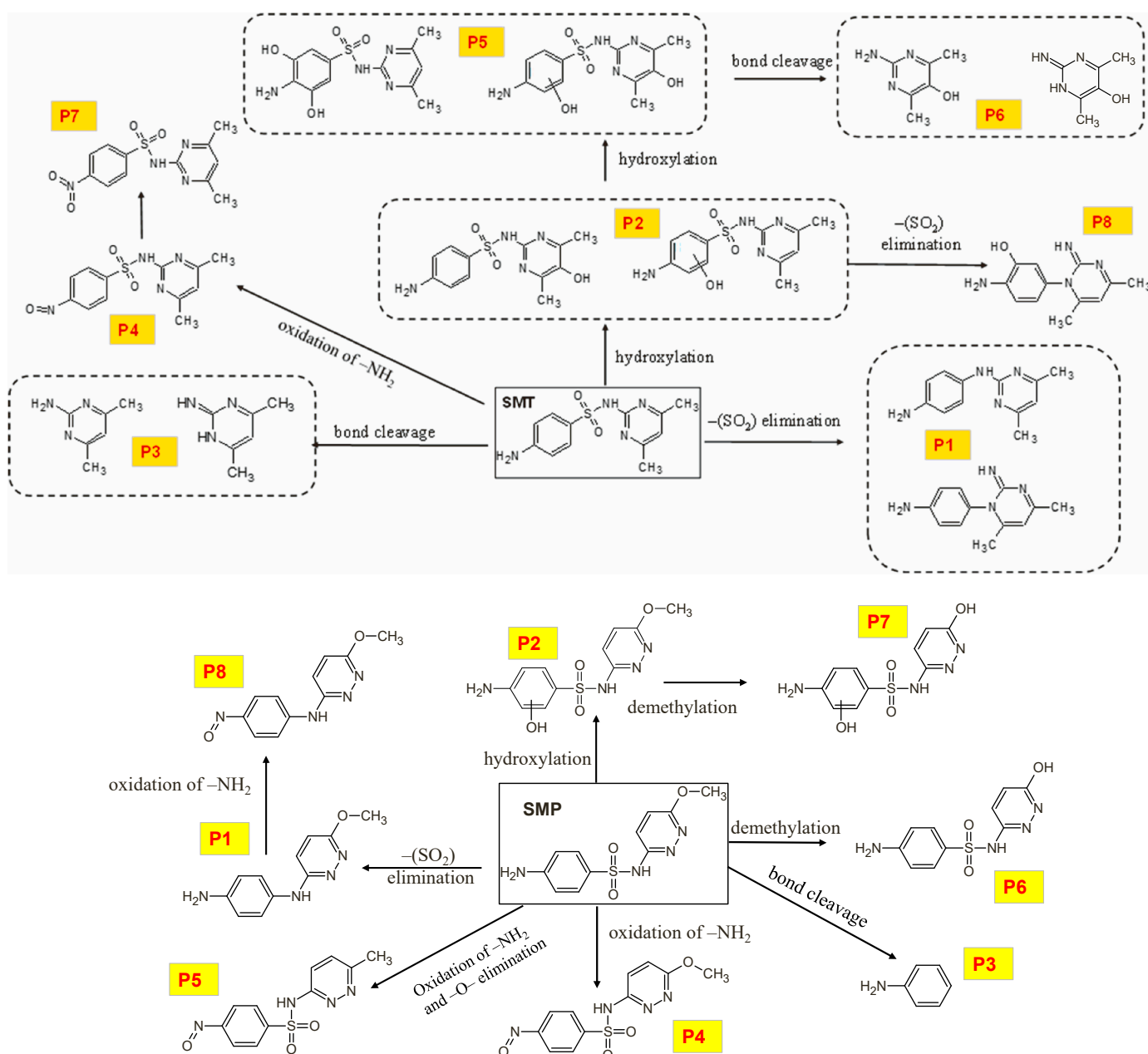


**Fig. 3.** The aromatic products detected during the transformation of SMT and SMP and the possible formation ways.

transformation way is influenced by $O_2$, likely via the ROS-initiated reaction [11,37].

The products can provide additional information to better understand the processes that occur in the case of various treatments. Several products have previously been identified in studies of the photolysis of sulfonamides [69,85,105], including SMP [32,50,69] and SMT [34]. The contribution of various processes (direct photolysis, photosensitization, and reaction with ROS) to the transformation and yield of photoproducts depends primarily on the structure of the heterocyclic ring and the substituents attached to the rings [69,93]. In addition to $-(SO_2)$ extrusion [18,37,50], other processes, such as bond breaking [105], hydroxylation [37,105] of the benzene ring (with less probability the heterocyclic ring), and ring opening process [93] also occur.

Products P1, P2, and P3 are formed upon UV photolysis of both sulfonamides (Fig. 4). (The retention times of the chromatographic peak of the products and the $m/z$ values are presented in Tables S4 and S5). The P1 product resulted through $-(SO_2)$ extrusion, which is a typical transformation way for the direct UV photolysis of sulfonamides [18,37,50]; however, to our knowledge, quantified data on this conversion have not been published so far. In this work, less than 40% of the S-content of the transformed SMT and SMP was detected as $SO_4^{2-}$ (Fig. S11). In addition to extrusion of $-(SO_2)$, products formed by hydroxylation (P2) and via cleavage of the N-S bond (P3 from SMT) and the C-S bond (P3 from SMP) were also identified (Fig. 3). Hydroxylated products (not detected in $O_2$-free solutions) support the additive role of ROS, however the moderated effect of $O_2$ on the conversion rate of sulfonamides confirms that, the significant way is the direct UV photolysis, even in aerated solutions. (Table 1 and Fig. S10).

The 40% $SO_4^{2-}$ yield, which does not increase even after sulfonamide decomposition (Fig. S11), suggests that although the $-(SO_2)$ extrusion is dominant in the transformation of SMT and SMP, it is not characteristic for the further transformation of S-containing products. The UV-resistant aromatic products of sulfonamides were also supposed by Voigt et al. [93] and confirmed by the slight decrease of the absorbance at 240 nm and around 260 nm (Fig S7 and S8). No more than $\sim$10% (SMT: 7 - 8%; SMP: 11 - 12%) of the N-content of target substances transformed to $NH_4^+$; its formation probably originated from $-NH_2$ moiety or $-NH-$ bridge. Formation of $NO_3^-$ or $NO_2^-$ were not observed (Fig. S11).

### 3.2. UV/VUV photolysis

Opposite to the UV photons absorbed by the target organic substances, 185 nm VUV photons are absorbed by water and generate $H^\bullet$ and $^\bullet OH$ ($\Phi(H^\bullet) = \Phi(^\bullet OH) = 0.33$ [39]) via bond dissociation of water molecules. The thickness of the irradiated aqueous solution layer (2.0 cm) ensures complete absorption of VUV photons [3,96]. Due to the additive effect of radical generation, the transformation rate is doubled compared to UV irradiated ones (Fig. 1.). Quantum yields for VUV photolysis of organic compounds are rarely published. Considering the flux of UV and VUV photons, the transformation rate of sulfonamides, and the $\sim$0.007 quantum efficiency of UV photolysis, the VUV light degrades the target molecules with $\sim$ 0.18 quantum efficiency. Li et al. [58] also published a 20-fold higher quantum yield for SMT VUV (185 nm) photolysis than for UV (254 nm) photolysis in a mini-fluidic UV/VUV photoreaction system.

The $^\bullet OH$ reacts with a high rate constant with both SMT ($6.95 \pm 1.69 \times 10^9$ $M^{-1}$ $s^{-1}$ [97] and $8.81 \pm 0.27 \times 10^9$ $M^{-1}$ $s^{-1}$ [108]) and SMP ($6.21 \pm 0.21 \times 10^9$ $M^{-1}$ $s^{-1}$ [108]). Dissolved $O_2$ reacts with $^\bullet H$ ($k(O_2 + ^\bullet H) = 1.2 \times 10^{10}$ $M^{-1}$ $s^{-1}$ [19]) and results in the formation $HO_2^\bullet$. The $HO_2^\bullet$ and the deprotonated ($pK_a = 4.8$ [13]) form ($O_2^{\bullet -}$) have much lower reactivity towards organic substances than $^\bullet OH$; instead of reacting with organic molecules, they recombine to $H_2O_2$. Dissolved $O_2$ generally promotes the transformation of organic matter, in part because peroxyl radicals [7] inhibit backward reactions and open new pathways for transformation. At the same time, while in an $O_2$-free solution, both $H^\bullet$ and $^\bullet OH$ can initiate the transformation via addition to aromatic ring or H-abstraction reactions, in the presence of $O_2$, $^\bullet OH$ is the primary reactant.

Although $O_2$ does not affect significantly the transformation rates (Fig. S10), it highly affects the change of the absorption spectra of UV/VUV treated solutions, indicating that the joint presence of $^\bullet OH$ and $O_2$ opens new pathways for the transformation of sulfonamides and their intermediates. In the case of UV photolysis, the dissolved $O_2$ slightly affected the change of spectra, as that was described previously. In $O_2$-free UV/VUV irradiated solutions, despite the doubled transformation rate of SMT and SMP (Table 1 and Fig S10), the change of spectra is similar to that observed for UV photolysis (Fig S7 and S8). This could be interpreted by the accumulation of aromatic intermediates. At the same time, in the case of UV/VUV photolysis of $O_2$-containing solutions, the absorbance at 260 and 230 nm decreases rapidly, which indicates a significant contribution of radical-based reactions and the importance of ring-opening processes in the transformation, preventing the accumulation of aromatic intermediates. The observations and explanations are consistent with the change in TOC values discussed later (Fig. 5).

The vital role of $^\bullet OH$-based reactions in the transformation of SMT, SMP [97,108] was confirmed by the amount of hydroxylated products (Fig. S12) and the radical scavenging effect of $t$-BuOH (Table 1). In addition to the products formed in UV-irradiated solutions, for SMT P4, P5, P6, P7 and P8, for SMP P4, P7 and P8 were detected. In the case of UV/VUV photolysis, the formation of hydroxylated product(s) (especially P2) became significant, obviously referring to the important role of $^\bullet OH$-based transformation. The concentration of the hydroxylated product P2 is highly enhanced by VUV photons (Fig S12) and changes according to the maximum curve. In addition to products formed by UV photolysis, new ones form through the oxidation of $-NH_2$ (P4, P7 from

**Table 1**

The effect of dissolved $O_2$ and $t$-BuOH, as $^\bullet OH$-scavenger on the transformation rate of SMT and SMP ($c_0^{SMT} = c_0^{SMP} = 1.0 \times 10^{-4}$ M and $c(O_3) = 1.3 \times 10^{-4}$ M).

| | | $r_0$ ($\times 10^{-8}$ M $s^{-1}$) | | | | | | | |
|---|---|---|---|---|---|---|---|---|---|
| | | UV | | UV/VUV | | $O_3$ | | $O_3$/UV | |
| | | SMT | SMP | SMT | SMP | SMT | SMP | SMT | SMP |
| aerated | | $3.20 \pm 0.14$ | $3.05 \pm 0.11$ | $6.33 \pm 0.93$ | $7.62 \pm 0.23$ | $30.7 \pm 2.16$ | $31.2 \pm 1.09$ | $32.0 \pm 0.63$ | $31.8 \pm 0.74$ |
| $O_2$-free | | $3.05 \pm 0.12$ | $2.98 \pm 0.14$ | $5.93 \pm 0.73$ | $7.37 \pm 0.51$ | - | - | - | - |
| | | $r_0^{\text{t-BuOH}}$ ($\times 10^{-8}$ M $s^{-1}$) | | | | | | | |
| | | SMT | SMP | SMT | SMP | SMT | SMP | SMT | SMP |
| $RSC_{\bullet OH}$ (%) | 50 | – | – | $5.55 \pm 0.73$ | $6.82 \pm 0.71$ | – | – | – | – |
| | 75 | – | – | $4.33 \pm 0.78$ | $4.93 \pm 0.85$ | – | – | – | – |
| | 98 | $3.00 \pm 0.22$ | $3.15 \pm 0.27$ | $3.08 \pm 0.17$ | $3.92 \pm 0.18$ | $28.5 \pm 1.18$ | $30.67 \pm 0.87$ | $33.00 \pm 0.59$ | $33.33 \pm 0.90$ |

$r_0$: initial transformation rate of SMT and SMP

$r_0^{\text{t-BuOH}}$: initial transformation rate of SMT and SMP in the presence of t-BuOH ($c_0^{\text{t-BuOH}} = 4.5 \times 10^{-4}$ M at 50% $RSC_{\bullet OH}$; $c_0^{\text{t-BuOH}} = 4.0 \times 10^{-3}$ M at 75% $RSC_{\bullet OH}$ and $c_0^{\text{t-BuOH}} = 6.0 \times 10^{-2}$ M at 98% $RSC_{\bullet OH}$)

$RSC_{\bullet OH}$: relative scavenging capacity of t-BuOH, determined in aerated solution

SMT and P4, P8 from SMP) [50,109] and bond cleavage (P6 from SMT) (Fig. 4).

The effect of *t*-BuOH as $^\bullet$OH-scavenger ($k_{t\text{-BuOH}} = 6.00 \times 10^8$ M$^{-1}$ s$^{-1}$ [19]) was investigated and characterized by relative scavenging capacity ($RSC_{\bullet OH}$) (Table 1):

$$RSC_{\bullet OH} = \frac{k_{t-BuOH} \times c_{t-BuOH}}{k_{t-BuOH} \times c_{t-BuOH} + k_{SA} \times c_{SA}} \times 100\%$$

where $c_{SA}$ and $c_{t\text{-BuOH}}$ are the initial concentrations of sulfonamide (SMT or SMP) ($c_{SA} = 1.0 \times 10^{-4}$ M) and *t*-BuOH. Based on the results, in addition to direct UV photolysis, the relative contribution of $^\bullet$OH-based reactions also became significant. In addition to t-BuOH, the effects of L-His, TEDA, FFA and HQ were also investigated and compared with their effects observed in the case of UV photolysis (Figs. S5, S6, and Table S2, and S3). The relative contribution of $^\bullet$OH-based reactions is 35%, similar for both SAs. VUV light does not affect the contribution of $^1O_2$-based transformation, its value is the same as that determined in UV-irradiated solutions (10%). In addition to $^\bullet$OH, $O_2^{\bullet-}$ plays a decisive role, and its contribution reaches 25% for SMP. The intensive transformation of organic substances is often accompanied by the enhanced $O_2^{\bullet-}$ formation, resulting in a higher contribution of $O_2^{\bullet-}$-based transformation of the parent compound (Table S3, Fig S6).

Compared to the UV photolysis, the $SO_4^{2-}$ yield is higher (about 60%) when SMT or SMP decomposed and reaches more than 90% conversion after 120 min of treatment indicating the intensive transformation of the S-containing UV-resistant products via radical-based reactions. The $NH_4^+$ and $NO_3^-$ yields also increased; almost 20% of N-contents were detected as the sum of $NH_4^+$ and $NO_3^-$. The $NO_3^-$ formation (Fig. S11) partly resulted in the oxidation of –NH$_2$ to –NO (SMT: P4 and SMP: P4, P5, P8) and –NO$_2$ moiety (P7 from SMT) (Fig. 4). The N-containing inorganic ions can also originate from the opening and fragmentation of N-containing rings.

### 3.3. Ozonation and its combination with UV photolysis

Ozone is a selective oxidizing agent that reacts with aromatic compounds with a wide range of second-order rate constants, depending on their structure and substituents [60]. As an electrophilic reaction partner, $O_3$ attacks the moieties of molecules with high electron density. Generally, $O_3$ reacts with sulfonamides with high rate constants (1.9 - 6.2 $\times 10^6$ M$^{-1}$ s$^{-1}$ [12,24,56,106]).

The transformation rate of SMT and SMP increased with the increase of both sulfonamide (1.0 $\times 10^{-5}$ – 1.0 $\times 10^{-4}$ M) and $O_3$ concentrations (1.3 $\times 10^{-4}$ – 3.2 $\times 10^{-4}$ M (in the gas phase)) (Fig. 4) in the investigated range. SMP was more sensitive to the $O_3$ concentration than SMT. The transformation rates demonstrate that ozonation is much more effective than UV or UV/VUV photolysis (Figs. 1 and 5; Table 1), even at low $O_3$ concentrations. Applying the lowest dose of $O_3$ (1.3 $\times 10^{-4}$ M in the gas

phase) and 1.0 $\times 10^{-4}$ M initial SMT/SMP concentration, the transformation was approximately ten times faster than under UV and 3–5 times higher than under UV/VUV irradiation (Table 1.).

During ozonation, the pH determines the dissolved $O_3$ and $^\bullet$OH concentrations. The $^\bullet$OH-initiated decomposition of $O_3$ results in $HO_2^\bullet$, $O_2^{\bullet-}$, and $^\bullet$OH. This chain reaction was described in the early 1980 s (SBH model, [38]) and became important at high pH values (pH > 10) and generally accelerates the transformation rate of organic substances due to the enhanced $^\bullet$OH concentration. In addition, the pH can influence the reaction rate with $O_3$ through the protonation of organic target substances. The results reported on the effect of pH during the ozonation of sulfonamides are somewhat contradictory. Some authors observed negligible or negative [43,61], while Garoma et al. [36] observed a slight positive effect of pH increase. In our cases, at pH 6 – 7, the main reaction partner is the $O_3$. The significant increase in the transformation rate was observed only at the highest pH of 10 for SMP (Fig. S2), which is probably related to the enhanced $^\bullet$OH generation.

Regardless of pH, 254 nm UV light increases the $^\bullet$OH concentration via direct reaction of O($^3$P) with water produces $^\bullet$OH and can enhance the transformation rate of organic substances in this way. This effect of UV radiation was not manifested in our cases; 254 nm radiation did not result in significant change, even at higher $O_3$ concentrations (Fig. 4b). Competition between sulfonamide and $O_3$ for 254 nm photons can reduce the efficiency of $^\bullet$OH generation. The effect of the $^\bullet$OH scavenger *t*-BuOH (Table 1) proved that the contribution of $^\bullet$OH-induced reactions to the transformation of sulfonamides is not significant in the case of UV/$O_3$, and the reaction with molecular $O_3$ remains dominant.

It should be noted that there is a significant difference between the reactivity of the aniline group and the N-containing rings towards $O_3$. The reaction of $O_3$ with the heterocyclic ring is much slower than with the aniline moiety [87,88]. In addition to the attack of the aniline group, $O_3$ can also react with the –NH bridge, –NH$_2$ and –CH$_3$ moieties [42]. Transformation can take place simultaneously, leading to hydroxylation of benzene moiety (P2 from SMT), oxidation of the amino group (P4 and P7 from SMT, P5 from SMP), demethylation (P6 from SMP), N-S and C–S bond cleavage (P3 from SMT) [42] (Fig. 3.). The reaction with the benzene ring most probably occurs via the well-known Criegee-mechanism and can result in both hydroxylated (P2 from SMT) and ring-opening products [42,94]. The –NH$_2$ moiety reacts with $O_3$ with less probability and results in nitrobenzene and nitrosobenzene (P4 and P7 from SMT, P5 from SMP). It is worth mentioning that the reaction of anilines with $O_3$ is accompanied by the formation of various radicals, even $^\bullet$OH [88], which highly accelerates the subsequent transformations.

Using ozonation or its combination with UV photolysis, the changes in spectra and the absorbance at the characteristic wavelengths (240 and ~260 nm) of the treated solutions are similar (Figs. S7, S8, and S9). The decrease in absorbance at 240 nm, which is related to the heterocyclic moiety, is much slower (Fig. S9) than that around 260 nm, reflecting the
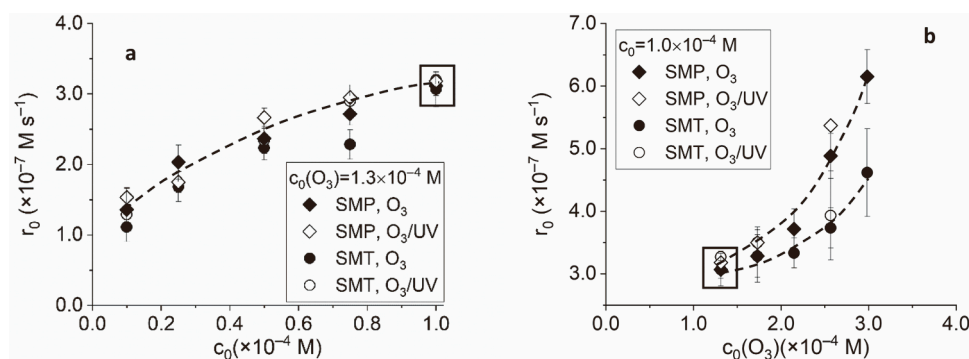


**Fig. 4.** Transformation rate of SMT and SMP in the case of ozonation and its combination with UV photolysis at various initial concentrations of sulfonamide (a) or ozone in the gas phase (b) (the framed point was measured at the same sulfonamide (1.0 $\times 10^{-4}$ M) and ozone (1.3 $\times 10^{-4}$ M) concentration).

lower reactivity of pyrimidine and pyridazine moieties towards $O_3$ [87]. In contrast to the $O_3$/UV and UV/VUV photolysis, the change in absorbance at 240 nm and 260 nm stopped after 20 min of ozonation in the case of SMT and significantly slowed down in the case of SMP, suggesting the formation of ozone-resistant aromatic products.

For ozonation, the $SO_4^{2-}$ yield does not exceed 75%, and the N-conversion into $NH_4^+$ and $NO_3^-$ (21–23%) is lower than for UV/VUV photolysis. The combination of ozonation with UV irradiation enhances the formation of inorganic ions; $SO_4^{2-}$ yield approaches 100%, and N-conversion into $NH_4^+$ and $NO_3^-$ was doubled (~40%).

## 3.4. Mineralization

The change in TOC value gives information about the mineralization efficiency. The S-content of the sulfonamides converts to $SO_4^{2-}$, while the N-content of molecules transforms to $NO_3^-$, $NH_4^+$, and $N_2$ as final products. The fate of organic N-content depends on the oxidation state of the N atom, its chemical environment, and the reaction parameters [10,74].

Mineralization of organic substances occurs through organic peroxyl radicals resulted in a fast reaction between carbon-centered radicals and $O_2$. Organic peroxyl radical may undergo a number of unimolecular processes; the most ubiquitous ones are $HO_2^\bullet$ and $O_2^{\bullet-}$ eliminations [7]. Consequently, the transformations, including the ring-opening process and fragmentation are followed by $HO_2^\bullet$ and $O_2^{\bullet-}$ formation. The formed $HO_2^\bullet$ and $O_2^{\bullet-}$ radicals having low reactivity towards organic substances - thus, during intensive mineralization, they accumulate and are primarily transformed by recombination, resulting in the formation of $H_2O_2$ ($k = 9.7 \times 10^7$ $M^{-1}$ $s^{-1}$) [14] Therefore, the accumulation of $H_2O_2$ (Fig. 5) is related to the intensity of the oxidative transformation of organic matter.

In UV-irradiated solutions, antibiotics decompose (Fig. S10) without changing the TOC value (Fig. 5), confirming that UV-resistant photoproducts of SMP and SMT remain in the solution. In UV/VUV irradiated ones, the decrease in TOC becomes intensive after the transformation of SMT or SMP, demonstrating the essential role of $^\bullet$OH in mineralization. In two hours, the TOC content was reduced by 65% (SMT) and 80% (SMP). The formation of inorganic ions (Fig. S10) and $H_2O_2$ is consistent with the decrease in TOC (Fig. 5). Compared to UV photolysis, in the case of UV/VUV photolysis, the $SO_4^{2-}$ yield doubled (SMT: 43% → 94% and SMP: 43% → 89%), and the conversion of the N-content of sulfonamides into $NO_3^-$ and $NH_4^+$ also increased (SMT: 12% → 37% and SMP: 8% → 38%), most likely because of the radical based transformation of N-containing rings. The change in $H_2O_2$ concentration reflects well the mineralization efficiency. In the case of UV photolysis, only a slow accumulation of $H_2O_2$ was observed ($c_{H2O2} < 5.0 \times 10^{-5}$ M). When UV/VUV treatment was applied, the $H_2O_2$ concentration varied, showing a maximum curve ($c_{H2O2}^{max} = 1.8 \times 10^{-4}$ M); its intensive formation and

decomposition occur together with the rapid decrease in TOC values (Fig. 5). However, a difference can be observed in the time dependence of $H_2O_2$ concentration between the sulfonamides. For SMT, the slow and prolonged $H_2O_2$ formation and decomposition indicate products that are more difficult to oxidize.

The fast reaction of $O_3$ with sulfonamides results in its transformation in 10 min; during this time, the decrease in TOC was 10%. After this short period, the TOC value becomes constant for SMT and reduction continues slowly for SMP, with a breakpoint at 60 min (Fig. 5). All this indicates the formation of products, which do not react (in the case of SMT) or react very slowly (in the case of SMP) with $O_3$. The first step is probably the prompt reaction of $O_3$ with the aniline moiety [87]. A multistep reaction yields ring-opening products inactive for further oxidation via $O_3$. Most likely, the difference manifested in the further change of TOC can be interpreted by the reactivity of $O_3$ to the substituted pyrimidine and pyridazine moiety [88] The $^\bullet$OH formation is negligible under the conditions applied in ozonation. The substituted pyrimidine moiety of SMT is practically inactive toward $O_3$ [88]. In the case of SMP, the further transformation of the products is possible via the addition of $O_3$ to the carbon-carbon double bond of the pyridazine moiety. In addition, $O_3$ preferentially attacks the N atoms and produces N-oxides [88]. The reaction of $O_3$ with organic compounds, depending on their structure, can be accompanied by the formation of $^\bullet$OH, promoting the transformation of products resistant to ozonation [88,94]. Although the role of $^\bullet$OH in the transformation of SMT and SMP during ozonation is negligible, its function can be decisive in the further fate of products that do not or slowly react with $O_3$. However, our results are insufficient to estimate and interpret the contribution of $^\bullet$OH to the mineralization in the case of simple ozonation. Ozonation is accompanied by a rapid increase in $H_2O_2$ concentration up to $5.0 \times 10^{-5}$ M during the first 10 min of the treatment in parallel with the transformation of sulfonamides and a decrease in TOC. The $H_2O_2$ concentration does not change afterward, consistent with inefficient or low-efficiency mineralization. During ozonation, 75% of the S-content was finally converted to $SO_4^{2-}$, while 21–23% of the N-content into the sum of the $NO_3^-$ and $NH_4^+$.

Although the combination of ozonation with UV did not affect the SMT and SMP transformation rate, it significantly enhanced mineralization and caused a 70–90% reduction in TOC in 60 min (Fig. 5). In this case, intermediates that are not reactive to ozone can be decomposed by $^\bullet$OH. The formation of inorganic ions (Fig. S11) was consistent with the decrease in TOC: S-content completely transformed into $SO_4^{2-}$ and almost 40% of N-content of sulfonamides was detected as the sum of $NO_3^-$ and $NH_4^+$; especially the $NO_3^-$ formation was enhanced. Both $^\bullet$OH or $O_3$ initiated transformation can result in $NO_2^-$, which can be easily converted to $NO_3^-$, especially in the presence of $^\bullet$OH ($k = 6.0 \times 10^9$ $M^{-1}$ $s^{-1}$ [63]) or $O_3$ ($k = 3.7 \times 10^5$ $M^{-1}$ $s^{-1}$ [47]), while oxidation of $NH_4^+$ to $NO_3^-$
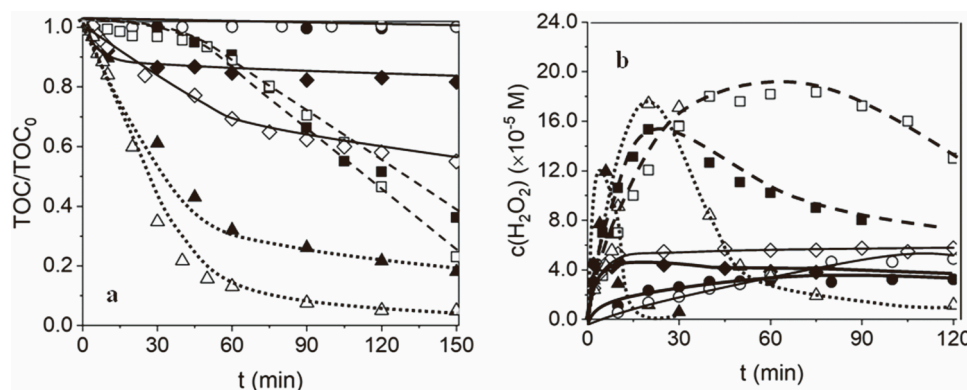


**Fig. 5.** The change in relative total organic carbon value (TOC/TOC$_0$) (a) and $H_2O_2$ concentration (b) versus time of treatment ($c_0^{SMT} = c_0^{SMP} = 1.0 \times 10^{-4}$ M; and c($O_3$) = $1.3 \times 10^{-4}$ M). ●: UV/air, SMT; ○: UV/air, SMP; ■: UV/VUV/air, SMT; □: UV/VUV/air, SMP; ◆: ozonation, SMT; ◇: ozonation, SMP; ▲: $O_3$/UV, SMT; △: $O_3$/UV, SMP.

is very slow. The $NO_3^-$ formation was not observed in the case of UV photolysis and was highly accelerated in the $O_3$/UV process compared to ozonation or UV/VUV methods (Fig. S11). Ozonation and $O_3$/UV combination were also performed at higher ($2.1 \times 10^{-4}$ M) $O_3$ concentration, but no further increase in mineralization rate was reached. It is also worth noting that in the case of SMT, almost 20% of TOC was not removed even after 150 min of $O_3$/UV treatment, while the complete mineralization of SMP takes place during this time. The $H_2O_2$ concentration showed a maximum curve (Fig. 5), and a higher maximum value of $H_2O_2$ concentration and more prolonged formation and decay were observed for SMP than for SMP.

### 3.5. Toxicity assays

#### 3.5.1. Ecotoxicity assay

Transformation of antibiotics can also result in biologically active products. The change in ecotoxicity was investigated via a bioluminescence test, which is based on the inhibition of light emitted by *Vibrio fisheri* bacteria. The ecotoxicity of the treated solutions increased during both UV and UV/VUV photolysis. However, the accumulation of organic products is characteristic only for UV photolysis, as evidenced by the change in the TOC value (Fig. 6). When ozonation was applied, the increase in toxicity was followed by its rapid decrease, and then became constant. Both the increased and residual toxicity effect may be related to organic products of UV photolysis and ozonation. The $O_3$/UV combination was the most effective in reducing ecotoxicity due to adequate mineralization. However, a characteristic difference can be observed between the two sulfonamides; in the case of SMP, the reduction in toxicity occurs much more slowly. For both sulfonamides, an increase in ecotoxicity was observed at the beginning of $O_3$/UV treatment.

The effect of inorganic ions should also be considered in addition to the potentially toxic organic products. The sensitivity of *Vibrio fisheri* to $NO_3^-$ and $NO_2^-$ was checked with $1.0 \times 10^{-4}$ M $NaNO_3$ and $NaNO_2$ solutions, but no significant effect was observed. Consequently, these ions cannot directly be responsible for the increase in toxicity. Nevertheless, under UV radiation, $NO_3^-$ can transform into $NO_2^-$ [84], which reacts with both $^\bullet$OH and $O_3$. Thus, the photochemical circulation between $NO_3^-$ and $NO_2^-$ in an aqueous solution, especially in the presence of oxidizing agents, such as $^\bullet$OH, $O_3$, $H_2O_2$, and (V)UV irradiation, is a very complex process [92] and accompanied by the formation of reactive N-containing species (RNS), such as $NO_3^\bullet$, $NO_2^\bullet$ and $NO^\bullet$ [78,82]. The secondary reactions that occur between RNS and organic substances can generate nitro-products, probably more toxic compared to the primary pollutants, and increase the toxicity of the treated solution. The lifetime of RNS exceeds that of ROS [73], which is partially responsible for the occurrence and importance of RNS-induced reactions despite the selectivity of RNS. It is also worth mentioning the synergism - the toxic effects caused by the individual components can significantly reinforce each other, so the effect caused by their simultaneous presence can far exceed the sum of the effects of the individual chemicals. Similar observations were made when the heterogeneous photocatalysis of imidacloprid and thiacloprid was compared [66]; the $NO_3^-$ formation was characteristic only of imidacloprid, and the formation of toxic nitro-derivatives was supposed.

#### 3.5.2. Change in the growth inhibition effect

Reducing antibacterial activity during treatment is essential to prevent the development of antibiotic-resistant bacterial strains. Primarily, the sulfanilamide moiety is responsible for the bacterial growth-inhibiting effect, so its transformation is decisive in terms of the biological activity of the products. $1.0 \times 10^{-4}$ M SMT and SMP solutions did not show activity against *E. coli* (results not shown), but inhibited the growth of *B. subtilis* and *M. luteus* bacterial cultures (Fig. 7). The effect decreased with decreasing sulfonamide concentration and disappeared below $5.0 \times 10^{-5}$ M.

The growth inhibition effect of treated samples decreased when UV or UV/VUV photolysis was applied, especially for SMP, in the case of UV/VUV photolysis. During ozonation, the inhibitory effect decreased with the reduction of the SMT concentration until its complete conversion; after that, it strengthened and became constant. All of this suggests that ozone-resistant products are biologically active and have growth-inhibitory effects. This trend was not observed for SMP; the inhibitory effect decreased during the treatments, although it did not completely disappear (Fig. 7). It is worth noting that ozonation was much more effective in reducing TOC for SMP than for SMT (Fig. 5). Similar to the ecotoxic tests, the $UV/O_3$ process proved to be the most effective.

Ozone is a selective oxidizing agent; therefore, when $O_3$ reacts with parts of molecules that are not critical for biochemical activity, products that have biological activity can form [27]. This ozone selectivity could be the reason of that, sulfamethoxazole results in products toxic to *Daphnia magna* and *Pseudokirchneriella subcapitata* [42], and the development of sulfonamide-resistant bacterial strains was observed [56] after ozonation. Our results emphasize that the transformation of sulfonamides is not sufficient in all cases to eliminate the ecological effect and prevent the development of strains resistant to antibacterial agents. Increased attention must also be paid to the biological impact of the products. The amount and chemical structure of the products depend on the reactive species, which are determined by the applied process. Further studies are necessary to focus on the biological activity of the products, especially in the case of UV photolysis and ozonation, where organic derivatives accumulate.
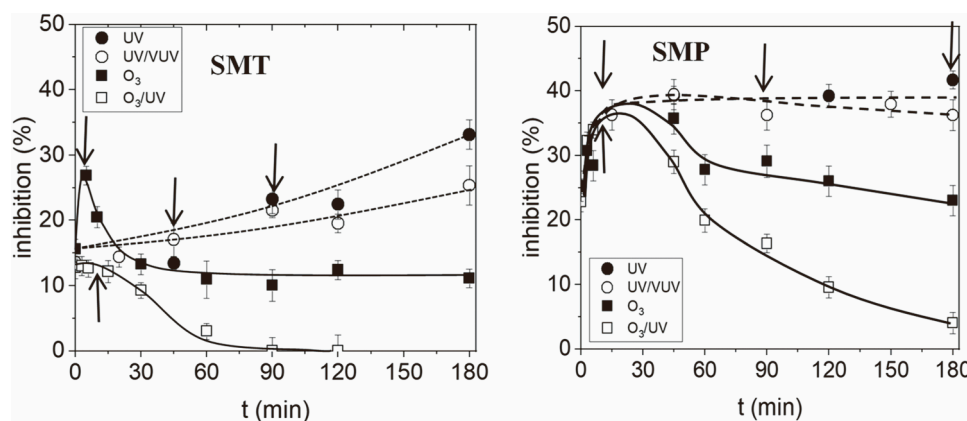


**Fig. 6.** The inhibition of bioluminescence as a function of time of treatment (arrows indicate the time of the 90% conversion of SMT and SMP) ($c_0^{SMT}= c_0^{SMP}=1.0 \times 10^{-4}$ M; and $c(O_3) = 1.3 \times 10^{-4}$ M).
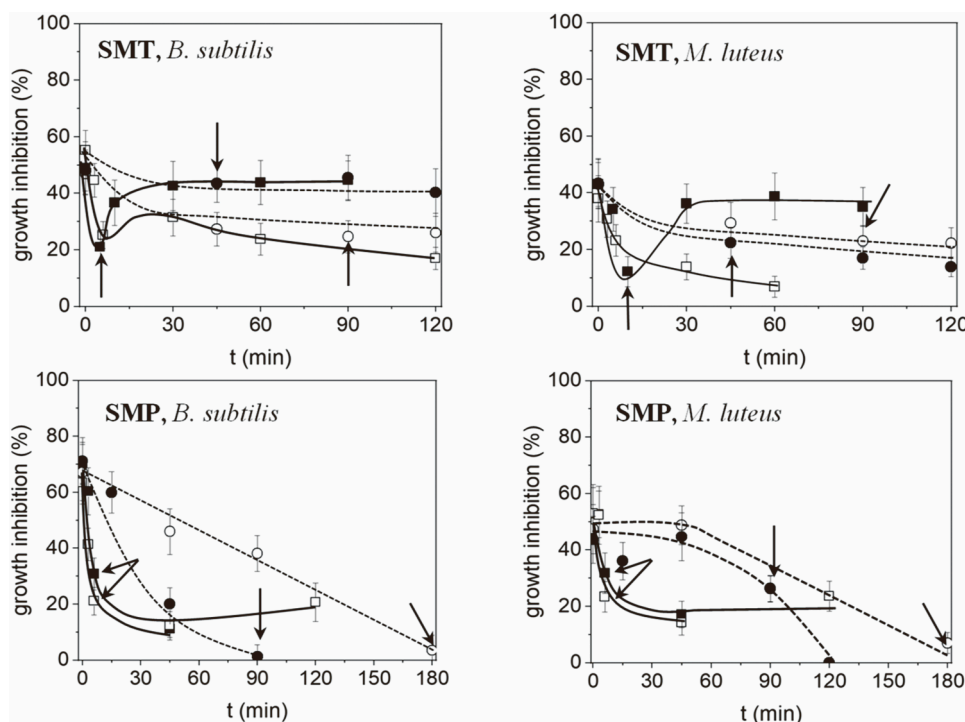
**Fig. 7.** The growth inhibition on *B. subtilis* and *M. luteus* as a function of treatment time (SMT: a and b; SMP: c and d) (arrows indicate complete conversion of SMT and SMP). ○: UV/air; ●: UV/VUV/air; ■: $O_3$; □: $O_3$/UV ($c_0^{SMT} = c_0^{SMP} = 1.0 \times 10^{-4}$ M; and $c(O_3) = 1.3 \times 10^{-4}$ M).

### 3.6. Energy efficiency − electrical energy per order

Electrical energy consumption ($E_{EO}$) required to operate the lamp and the ozonizer to decrease the concentration from $1.0 \times 10^{-4}$ M to $1.0 \times 10^{-5}$ M was calculated and compared (Fig. S13). The lowest value was obtained for ozonation (2.9 and 3.8 kWh m$^{-3}$ order$^{-1}$). The increase in $O_3$ concentration ($1.3 \times 10^{-4} \rightarrow 1.7 \times 10^{-4}$ M) caused a slightly faster conversion and doubled the $E_{EO}$ value. Thus, the application of a lower $O_3$ concentration is more economical. Combining ozonation with UV light increased $E_{EO}$ values by 40 – 50%. However, it is worth considering that, although ozonation is highly effective in removing SMT and SMP, the treated solution contains several non-ozone-reactive intermediates whose biological effects are unknown. The ecotoxicity of the resulting multicomponent solution is comparable to that of the starting solutions (Figs. 6 and 7) and may have a bacterial-growth inhibition effect. Consequently, the reduction of the ecotoxicity effect and the elimination of the bacterial growth inhibition effect require two or three times longer treatment time and correspondingly higher energy demand than the simple removal of sulfonamides, even in the case of the $O_3$/UV process.

### 4. Summary

Four processes, UV (254 nm) and UV/VUV (254/185 nm) photolysis, ozonation, and $O_3$/UV (254 nm) combination, were compared for the transformation of sulfamethazine (SMT) and sulfamethoxypyridazine (SMP) antibiotics. UV photolysis was moderately effective in transforming both sulfonamides, and the accumulation of their products was observed. The UV/VUV irradiation doubled the transformation rate and significantly enhanced mineralization due to the $\bullet$OH-based reactions. Taking into account the photon flux at 254 and 185 nm, the apparent quantum efficiency of UV photolysis (~0.007) is significantly lower than that of VUV photolysis (<0.15). The relative contribution of reaction with $\bullet$OH, $^1O_2$ and $O_2^{\bullet-}$ were determined in UV and UV/VUV irradiated solutions. In addition to UV photolysis and $\bullet$OH-based reactions, the $O_2^{\bullet-}$ have important role in the transformation of SAs.

When ozonation is applied, transformation rates are ten times higher than under UV irradiation, even at low ($1.3 \times 10^{-4}$ M) $O_3$ dosage. The $O_3$/UV combination does not improve the transformation rates. However, the intense reduction of TOC in the $O_3$/UV process underscores the importance of $\bullet$OH-based reactions in transforming products. This is highly important since *V. fisheri* tests and bacteria growth inhibition tests indicated the formation of products that have biological activity after ozonation and UV photolysis. The $O_3$/UV process can eliminate these effects. The formation of $NO_3^-$ in the case of $O_3$ or $\bullet$OH driven processes (ozonation, UV/VUV photolysis, and $O_3$/UV process) can be associated with the formation of nitro-derivatives and consequently, the increase in toxicity. Our results showed a correlation between the reactivity of nitrogen-containing moieties with $O_3$, the rate of mineralization, and the change in ecotoxicity and bacterial growth inhibition effect of the treated solutions.

The $E_{EO}$ values showed that ozonation is the most cost-effective method for the decomposition of both SMT and SMP, even at low $O_3$ concentrations. Combining ozonation with UV photolysis increases electrical energy consumption by 40 – 50%. However, the $O_3$/UV process is recommended due to the efficient conversion of the biologically active products of ozonation, ecotoxicity reduction, and the complete elimination of the residual bacterial grown inhibition effect. Our work emphasizes the need for a toxicological characterization of treated samples since removal of the parent compound is not enough to avoid the release of toxic species into the environment.

### CRediT authorship contribution statement

**Tünde Alapi:** Conceptualization, supervision, Writing - Original Draft, Review & Editing, Supervision, Funding acquisition. **Luca Farkas:** Investigation and Formal Analysis, Visualization, Writing - Original Draft, Review & Editing. **Ilaria Monzini:** Investigation. **Erzsébet Takács:** Writing - Original Draft, Review & Editing. **László Wojnárovits:** Writing - Original Draft, Review & Editing. **Mónika Vörös:** Investigation (Bacterial growth inhibition test). **Csaba Vágvölgyi:** Resources, Methodology. **Csaba Janáky:** Resources,

Methodology.

## Declaration of Competing Interest

The authors declare that they have no known competing financial interests or personal relationships that could have appeared to influence the work reported in this paper.

## Data availability

Data will be made available on request.

## Acknowledgment

## Appendix A. Supporting information

Supplementary data associated with this article can be found in the online version at doi:10.1016/j.jece.2023.111845.

## References

[1] T. Aissani, I. Yahiaoui, F. Boudrahem, S.A. Chikh, A. Amrane, The combination of photocatalysis process ( UV / TiO 2 ( P25) and UV / ZnO) with activated sludge culture for the degradation of sulfamethazine, Sep. Sci. Technol. 00 (2018) 1–11, https://doi.org/10.1080/01496395.2018.1445109.

[2] M.Z. Akbari, Y. Xu, Z. Lu, L. Peng, Review of antibiotics treatment by advance oxidation processes, Environ. Adv. 5 (2021) 100111, https://doi.org/10.1016/j.envadv.2021.100111.

[3] S. Al-Gharabli, P. Engeßer, D. Gera, S. Klein, T. Oppenländer, Engineering of a highly efficient Xe2*-excilamp (xenon excimer lamp, λmax=172 nm, η=40%) and qualitative comparison to a low-pressure mercury lamp (LP-Hg, λ=185/254 nm) for water purification, Chemosphere 144 (2016) 811–815, https://doi.org/10.1016/j.chemosphere.2015.09.012.

[4] A.A. Al-Suhybani, G. Hughes, Pulse radiolysis of deaerated hydroquinone solutions, J. Chem. Soc. Pak. 8 (1986) 107–115.

[5] A. Al Hoque, C. Guha, N. Sepay, S.P. Dey, U.C. Halder, Anti-COVID-19 Sulfonamides: A DFT, Docking and ADMET Study, Coronaviruses 3 (2022), https://doi.org/10.2174/2666796702666210719103409.

[6] T. Alapi, K. Schrantz, E.E. Arany, Z. Kozmér, Vacuum UV radiation-driven processes, : Mihaela I. Stefan (Ed. ), Adv. Oxid. Process. Water Treat. IWA Publ. (2017) 195–241, https://doi.org/10.2166/9781780407197_0195.

[7] Z.B. Alfassi. Peroxyl Radicals in Aqueous Solutions, in the Chemistry of Free Radicals: Peroxyl Radicals, 1st ed.,, Wiley-Blackwell Publishing Ltd,, New Jersey, 1997.

[8] H.Q. Anh, T.P.Q. Le, N. Da Le, X.X. Lu, T.T. Duong, J. Garnier, E. Rochelle-Newall, S. Zhang, N.-H. Oh, C. Oeurng, C. Ekkawatpanit, Tien Dat Nguyen, Q. T. Nguyen, Nguyen, Dung Tran, T.N. Nguyen, T.L. Tran, T. Kunisue, R. Tanoue, S. Takahashi, T.B. Minh, H.T. Le, T.N.M. Pham, T.A.H. Nguyen, Antibiotics in surface water of East and Southeast Asian countries: A focused review on contamination status, pollution sources, potential risks, and future perspectives, Sci. Total Environ. 764 (2021) 142865, https://doi.org/10.1016/j.scitotenv.2020.142865.

[9] C. Baeza, D.R.U. Knappe, Transformation kinetics of biochemically active compounds in low-pressure UV Photolysis and UV/H2O2 advanced oxidation processes, Water Res 45 (2011) 4531–4543, https://doi.org/10.1016/j.watres.2011.05.039.

[10] D. Bamba, M. Coulibaly, D. Robert, Nitrogen-containing organic compounds: Origins, toxicity and conditions of their photocatalytic mineralization over TiO2, Sci. Total Environ. 580 (2017) 1489–1504, https://doi.org/10.1016/j.scitotenv.2016.12.130.

[11] A.P.S. Batista, F.C.C. Pires, A.C.S.C. Teixeira, Photochemical degradation of sulfadiazine, sulfamerazine and sulfamethazine: Relevance of concentration and heterocyclic aromatic groups to degradation kinetics, J. Photochem. Photobiol. A Chem. 286 (2014) 40–46, https://doi.org/10.1016/j.jphotochem.2014.04.022.

[12] W. Ben, Z. Qiang, X. Pan, Y. Nie, Degradation of Veterinary Antibiotics by Ozone in Swine Wastewater Pretreated with Sequencing Batch Reactor, J. Environ. Eng. 138 (2012) 272–277, https://doi.org/10.1061/(ASCE)EE.1943-7870.0000404.

[13] B.H.J. Bielski, Reevaluation of the Spectral and Kinetic Properties of Ho2 and O2-Free Radicals, Photochem. Photobiol. 28 (1978) 645–649, https://doi.org/10.1111/j.1751-1097.1978.tb06986.x.

[14] B.H.J. Bielski, D.E. Cabelli, R.L. Arudi, A.B. Ross, Reactivity of HO 2 /O − 2 Radicals in Aqueous Solution, J. Phys. Chem. Ref. Data 14 (1985) 1041–1100, https://doi.org/10.1063/1.555739.

[15] M. Biošić, M. Mitrevski, S. Babić, Environmental behavior of sulfadiazine, sulfamethazine, and their metabolites, Environ. Sci. Pollut. Res. 24 (2017) 9802–9812, https://doi.org/10.1007/s11356-017-8639-8.

[16] B.T.P.Van Boeckel, Glennon, E. Emma, D. Chen, M. Gilbert, T.P. Robinson, B. T. Grenfell, S.A. Levin, S. Bonhoeffer, Reducing antimicrobial use in food animals, Insigths 357 (2017) 2–5.

[17] J.R. Bolton, K.G. Bircher, W. Tumas, C.A. Tolman, Figures-of-merit for the technical development and application of advanced oxidation technologies for both electric- and solar-driven systems, Pure Appl. Chem. 73 (2001) 627–637, https://doi.org/10.1351/pac200173040627.

[18] A.L. Boreen, W.A. Arnold, K. McNeill, Triplet-Sensitized Photodegradation of Sulfa Drugs Containing Six-Membered Heterocyclic Groups: Identification of an SO 2 Extrusion Photoproduct, Environ. Sci. Technol. 39 (2005) 3630–3638, https://doi.org/10.1021/es048331p.

[19] G.V. Buxton, C.L. Greenstock, W.P. Helman, A.B. Ross, Critical Review of rate constants for reactions of hydrated electrons, hydrogen atoms and hydroxyl radicals (·OH/·O − in Aqueous Solution, J. Phys. Chem. Ref. Data 17 (1988) 513–886, https://doi.org/10.1063/1.555805.

[20] I.T. Carvalho, L. Santos, Antibiotics in the aquatic environments: A review of the European scenario, Environ. Int. (2016), https://doi.org/10.1016/j.envint.2016.06.025.

[21] A. Cassini, L.D. Högberg, D. Plachouras, A. Quattrocchi, A. Hoxha, Attributable deaths and disability-adjusted life-years caused by infections with antibiotic-resistant bacteria in the EU and the European Economic Area in 2015: a population-level modelling analysis, Lancet Infect. Dis. (2019), https://doi.org/10.1016/S1473-3099(18)30605-4.

[22] J.K. Challis, J.C. Carlson, K.J. Friesen, M.L. Hanson, C.S. Wong, Aquatic photochemistry of the sulfonamide antibiotic sulfapyridine, J. Photochem. Photobiol. A Chem. 262 (2013) 14–21, https://doi.org/10.1016/j.jphotochem.2013.04.009.

[23] L. Charuaud, E. Jarde, A. Jaffrezic, M.-F.F. Thomas, B. Le Bot, Veterinary pharmaceutical residues from natural water to tap water: Sales, occurrence and fate, J. Hazard. Mater. 361 (2019) 169–186, https://doi.org/10.1016/j.jhazmat.2018.08.075.

[24] L.C. Chuang, C.H. Luo, S.W. Huang, C.J. Lin, Degradation of sulfa pharmaceuticals in aquatic environment by O 3 and UV/TiO2 processes, Adv. Mater. Res. 255–260 (2011) 4222–4226, https://doi.org/10.4028/www.scientific.net/AMR.255-260.4222.

[25] M. Conde-Cid, D. Fernández-Calviño, J.C. Nóvoa-muñoz, M. Arias-estévez, M. Díaz-Raviña, A. Núñez-Delgado, M.J. Fernández-Sanjurjo, E. Álvarez-Rodríguez, Degradation of sulfadiazine, sulfachloropyridazine and sulfamethazine in aqueous media, J. Environ. Manag. 228 (2018) 239–248, https://doi.org/10.1016/j.jenvman.2018.09.025.

[26] M. Conde-Cid, A. Núñez-Delgado, M. Fernández-Sanjurjo, E. Álvarez-Rodríguez, D. Fernández-Calviño, M. Arias-Estévez, Tetracycline and Sulfonamide Antibiotics in Soils: Presence, Fate and Environmental Risks, Processes 8 (2020) 1479, https://doi.org/10.3390/pr8111479.

[27] M.C. Dodd, M.O. Buffle, U. Von Gunten, Oxidation of antibacterial molecules by aqueous ozone: Moiety-specific reaction kinetics and application to ozone-based wastewater treatment, Environ. Sci. Technol. 40 (2006) 1969–1977, https://doi.org/10.1021/es051369x.

[28] A.B. Falowo, O. Festus Akimoladun, Veterinary Drug Residues in Meat and Meat Products: Occurrence, Detection and Implications, Vet. Med. Pharm. (2020), https://doi.org/10.5772/intechopen.83616.

[29] A. Fischbacher, L.H. V, T.C. Schmidt, Ozone/H2O2 and ozone/UV processes, in: I. M. Stefan (Ed.), Advanced Oxidation Processes for Water Treatment: Fundamentals and Applications, IWA Publishing, London, 2017, pp. 163–195.

[30] Franklin Vargas, J. Hisbeth Mendez, PHOTOTOXICITY INDUCED BY 1O2 GENERATION DURING THE PHOTODEGRADATION OF SOME DIURETIC DRUGS, Toxic. Subst. Mech. 18 (1999) 53–65, https://doi.org/10.1080/107691899229142.

[31] C. Fu, B. Xu, H. Chen, X. Zhao, G. Li, Y. Zheng, W. Qiu, C. Zheng, L. Duan, W. Wang, Occurrence and distribution of antibiotics in groundwater, surface water, and sediment in Xiong'an New Area, China, and their relationship with antibiotic resistance genes, Sci. Total Environ. 807 (2022) 151011, https://doi.org/10.1016/j.scitotenv.2021.151011.

[32] Y. qiong Gao, N. yun Gao, W. hai Chu, Y. feng Zhang, J. Zhang, D. qiang Yin, UV-activated persulfate oxidation of sulfamethoxypyridazine: Kinetics, degradation pathways and impact on DBP formation during subsequent chlorination, Chem. Eng. J. 370 (2019) 706–715, https://doi.org/10.1016/j.cej.2019.03.237.

[33] Y. qiong Gao, N. yun Gao, Y. Deng, Y. qiong Yang, Y. Ma, Y. qiong Gao, N. yun Gao, Y. Deng, Y. qiong Yang, Y. Ma, Y. qiong Gao, N. yun Gao, Y. Deng, Y. qiong Yang, Y. Ma, Ultraviolet (UV) light-activated persulfate oxidation of sulfamethazine in water, Chem. Eng. J. 195–196 (2012) 248–253, https://doi.org/10.1016/j.cej.2012.04.084.

[34] M.J. García-Galán, M.S. Díaz-Cruz, D. Barceló, Kinetic studies and characterization of photolytic products of sulfamethazine, sulfapyridine and their acetylated metabolites in water under simulated solar irradiation, Water Res 46 (2012) 711–722, https://doi.org/10.1016/j.watres.2011.11.035.

[35] M.J.M.J. García-Galán, M. Silvia Díaz-Cruz, D. Barceló, Identification and determination of metabolites and degradation products of sulfonamide antibiotics, TrAC Trends Anal. Chem. 27 (2008) 1008–1022, https://doi.org/10.1016/j.trac.2008.10.001.

[36] T. Garoma, S.K. Umamaheshwar, A. Mumper, Chemosphere Removal of sulfadiazine, sulfamethizole, sulfamethoxazole, and sulfathiazole from aqueous solution by ozonation, Chemosphere 79 (2010) 814–820, https://doi.org/10.1016/j.chemosphere.2010.02.060.

[37] L. Ge, P. Zhang, C. Halsall, Y. Li, C.E. Chen, J. Li, H. Sun, Z. Yao, The importance of reactive oxygen species on the aqueous phototransformation of sulfonamide antibiotics: kinetics, pathways, and comparisons with direct photolysis, Water Res 149 (2019) 243–250, https://doi.org/10.1016/j.watres.2018.11.009.

[38] D. Gerrity, F.L. Rosario-Ortiz, E.C. Wert, Application of ozone in water and wastewater treatment, in: I.M. Stefan (Ed.), Advanced Oxidation Processes for Water Treatment: Fundamentals and Applications, IWA Publishing, London, 2017, pp. 123–163.

[39] N. Getoff, G.O. Schenck, Primary products of liquid water photolysis at 1236, 1470 and 1849 Å, Photochem. Photobiol. 8 (1968) 167–178.

[40] G.A.S. Gireli, M.G. Maniero, J.R. Guimarães, Influence of pH value on sulfonamide ozonation using caffeine as a contamination indicator, Water Sci. Technol. Water Supply 20 (2020) 508–515, https://doi.org/10.2166/ws.2019.182.

[41] A. Gome, K. Upadhyay, Chemical kinetics of ozonation and other processes used for the treatment of wastewater containing, Pharmaceuticals: A Rev. 04 (2012) 157–168.

[42] M. del M. Gómez-Ramos, M. Mezcua, A. Agüera, A.R. Fernández-Alba, S. Gonzalo, A. Rodríguez, R. Rosal, Chemical and toxicological evolution of the antibiotic sulfamethoxazole under ozone treatment in water solution, J. Hazard. Mater. 192 (2011) 18–25, https://doi.org/10.1016/j.jhazmat.2011.04.072.

[43] W. Guo, Z. Yang, J. Du, R. Yin, X. Zhou, S. Jin, N. Ren, Degradation of sulfadiazine in water by a UV/O 3 process: performance and degradation pathway, RSC Adv. 6 (2016) 57138–57143, https://doi.org/10.1039/C6RA09078H.

[44] W.R. Haag, J. Hoigné, E. Gassman, A. Braun, Singlet oxygen in surface waters — Part I: Furfuryl alcohol as a trapping agent, Chemosphere 13 (1984) 631–640, https://doi.org/10.1016/0045-6535(84)90199-1.

[45] C.G. Hatchard, C.A. Parker, H. Heath, C.G. Hatchard, C.A. Parker, A new sensitive chemical actinometer - II. Potassium ferrioxalate as a standard chemical actinometer, Proc. R. Soc. Lond. Ser. A. Math. Phys. Sci. 235 (1956) 518–536, https://doi.org/10.1098/rspa.1956.0102.

[46] T.H. Ho, C.H. Wu, T.Y. Han, W.J. Syu, Mineralization of sulfonamides from wastewater using ozone-based systems, Water Sci. Technol. 84 (2021) 1379–1388, https://doi.org/10.2166/wst.2021.325.

[47] Hoigné, J., 1998, Chemistry of Aqueous Ozone and Transformation of Pollutants by Ozonation and Advanced Oxidation Processes. pp. 83–141. https://doi.org/10.1007/978-3-540-68089-5_5.

[48] H. Hou, L. Duan, B. Zhou, Y. Tian, J. Wei, F. Qian, The performance and degradation mechanism of sulfamethazine from wastewater using IFAS-MBR, Chin. Chem. Lett. 31 (2020) 543–546, https://doi.org/10.1016/j.cclet.2019.08.031.

[49] J. Huang, J. Liang, X. Yang, J. Zhou, X. Liao, S. Li, L. Zheng, S. Sun, Ultrasonic coupled bioleaching pretreatment for enhancing sewage sludge dewatering: Simultaneously mitigating antibiotic resistant genes and changing microbial communities, Ecotoxicol. Environ. Saf. 193 (2020) 110349, https://doi.org/10.1016/j.ecoenv.2020.110349.

[50] N.D.H.H. Khaleel, W.M.M.M. Mahmoud, G.M. Hadad, R.A. Abdel-Salam, K. Kümmerer, Photolysis of sulfamethoxypyridazine in various aqueous media: Aerobic biodegradation and identification of photoproducts by LC-UV-MS/MS, J. Hazard. Mater. 244–245 (2013) 654–661, https://doi.org/10.1016/j.jhazmat.2012.10.059.

[51] H.Y. Kim, T.H. Kim, S. Yu, Photolytic degradation of sulfamethoxazole and trimethoprim using UV-A, UV-C and vacuum-UV (VUV), J. Environ. Sci. Heal. - Part A Toxic. /Hazard. Subst. Environ. Eng. 50 (2015) 292–300, https://doi.org/10.1080/10934529.2015.981118.

[52] H.Y. Kim, S.H. Yu, M.J. Lee, T.H. Kim, S.D. Kim, Radiolysis of selected antibiotics and their toxic effects on various aquatic organisms, Radiat. Phys. Chem. 78 (2009) 267–272, https://doi.org/10.1016/j.radphyschem.2009.01.010.

[53] I. Kraljić, V.A. Sharpatyi, Determination of singlet oxygen rate constants in aqueous solutions, Photochem. Photobiol. 28 (1978) 583–586, https://doi.org/10.1111/j.1751-1097.1978.tb06973.x.

[54] M. Kumar, S. Jaiswal, K.K. Sodhi, P. Shree, D.K. Singh, P.K. Agrawal, P. Shukla, Antibiotics bioremediation: Perspectives on its ecotoxicity and resistance, Environ. Int. 124 (2019) 448–461, https://doi.org/10.1016/j.envint.2018.12.065.

[55] R.R. Kumar, J.T. Lee, J.Y. Cho, Fate, occurrence, and toxicity of veterinary antibiotics in environment, J. Korean Soc. Appl. Biol. Chem. 55 (2012) 701–709, https://doi.org/10.1007/S13765-012-2220-4.

[56] G. Li, W. Ben, H. Ye, D. Zhang, Z. Qiang, Performance of ozonation and biological activated carbon in eliminating sulfonamides and sulfonamide-resistant bacteria: A pilot-scale study, Chem. Eng. J. 341 (2018) 327–334, https://doi.org/10.1016/j.cej.2018.02.035.

[57] M. Li, W. Li, J.R. Bolton, E.R. Blatchley, Z. Qiang, Organic Pollutant Degradation in Water by the Vacuum-Ultraviolet/Ultraviolet/H 2 O 2 Process: Inhibition and Enhancement Roles of H 2 O 2, Environ. Sci. Technol. 53 (2019) 912–918, https://doi.org/10.1021/acs.est.8b05831.

[58] M. Li, C. Wang, M. Yau, J.R. Bolton, Z. Qiang, Sulfamethazine degradation in water by the VUV/UV process: Kinetics, mechanism and antibacterial activity determination based on a mini-fluidic VUV/UV photoreaction system, Water Res 108 (2017) 348–355, https://doi.org/10.1016/j.watres.2016.11.018.

[59] Y. Li, X. Wei, J. Chen, H. Xie, Y. nan Zhang, Photodegradation mechanism of sulfonamides with excited triplet state dissolved organic matter: A case of sulfadiazine with 4-carboxybenzophenone as a proxy, J. Hazard. Mater. 290 (2015) 9–15, https://doi.org/10.1016/j.jhazmat.2015.02.040.

[60] S. Lim, J.L. Shi, U. von Gunten, D.L. McCurry, Ozonation of organic compounds in water and wastewater: A critical review, Water Res 213 (2022) 118053, https://doi.org/10.1016/j.watres.2022.118053.

[61] A.Y.-C. Lin, C.-F. Lin, J.-M. Chiou, P.K.A. Hong, O3 and O3/H2O2 treatment of sulfonamide and macrolide antibiotics in wastewater, J. Hazard. Mater. 171 (2009) 452–458, https://doi.org/10.1016/j.jhazmat.2009.06.031.

[62] Y. Lion, E. Gandin, A. Van de Vorst, On the production of nitroxide radicals by singlet oxygen reaction: an EPR study, Photochem. Photobiol. 31 (1980) 305–309, https://doi.org/10.1111/j.1751-1097.1980.tb02545.x.

[63] T. Loegager, K. Sehested, T. Løgager, K. Sehested, Formation and decay of peroxynitric acid: A pulse radiolysis study, J. Phys. Chem. 97 (1993) 10047–10052, https://doi.org/10.1021/j100141a025.

[64] C.A. Morales-Paredes, J.M. Rodríguez-Díaz, N. Boluda-Botella, Pharmaceutical compounds used in the COVID-19 pandemic: A review of their presence in water and treatment techniques for their elimination, Sci. Total Environ. 814 (2022), https://doi.org/10.1016/j.scitotenv.2021.152691.

[65] T.W. Na, T.W. Kang, K.H. Lee, S.H. Hwang, H.J. Jung, K. Kim, Distribution and ecological risk of pharmaceuticals in surface water of the Yeongsan river, Republic of Korea, Ecotoxicol. Environ. Saf. 181 (2019) 180–186, https://doi.org/10.1016/j.ecoenv.2019.06.004.

[66] M. Náfrádi, T. Alapi, G. Bencsik, C. Janáky, Impact of Reaction Parameters and Water Matrices on the Removal of Organic Pollutants by TiO2/LED and ZnO/LED Heterogeneous Photocatalysis Using 365 and 398 nm Radiation, Nanomaterials 12 (2021) 5, https://doi.org/10.3390/nano12010005.

[67] M. Náfrádi, T. Alapi, L. Farkas, G. Bencsik, G. Kozma, K. Hernádi, Wavelength Dependence of the Transformation Mechanism of Sulfonamides Using Different LED Light Sources and TiO2 and ZnO Photocatalysts, Mater. (Basel) 15 (2021) 49, https://doi.org/10.3390/ma15010049.

[68] M. Náfrádi, K. Hernadi, Z. Kónya, T. Alapi, Investigation of the efficiency of BiOI/BiOCl composite photocatalysts using UV, cool and warm white LED light sources - Photon efficiency, toxicity, reusability, matrix effect, and energy consumption, Chemosphere 280 (2021) 130636, https://doi.org/10.1016/j.chemosphere.2021.130636.

[69] R. Nassar, A. Trivella, S. Mokh, M. Al-iskandarani, H. Budzinski, P. Mazellier, Photodegradation of sulfamethazine, sulfamethoxypiridazine, amitriptyline, and clomipramine drugs in aqueous media, J. Photochem. Photobiol. A Chem. 336 (2017) 176–182, https://doi.org/10.1016/j.jphotochem.2016.12.008.

[70] T. Oppenländer, R. Schwarzwalder, Vacuum-UV Oxidation (H2O-VUV) with a Xenon Excimer Flow-Trough Lamp at 172 nm: Use of Methanol as Actinometer for VUV Intensity Measurement and as Reference Compound for OH-Radical Competition Kinetics in Aqueous Systems, J. Adv. Oxid. Technol. 5 (2002), https://doi.org/10.1515/jaots-2002-0205.

[71] H. Park, Y. Park, W. Kim, W. Choi, Surface modification of TiO2 photocatalyst for environmental applications, J. Photochem. Photobiol. C Photochem. Rev. 15 (2013) 1–20, https://doi.org/10.1016/j.jphotochemrev.2012.10.001.

[72] M.R. Perry, H.C. Lepper, L. McNally, B.A. Wee, P. Munk, A. Warr, B. Moore, P. Kalima, C. Philip, A.M. de Roda Husman, F.M. Aarestrup, M.E.J.J. Woolhouse, B.A.D.D. van Bunnik, Secrets of the Hospital Underbelly: Patterns of Abundance of Antimicrobial Resistance Genes in Hospital Wastewater Vary by Specific Antimicrobial and Bacterial Family, Front. Microbiol. 12 (2021), https://doi.org/10.3389/fmicb.2021.703560.

[73] A. Phaniendra, D.B. Jestadi, L. Periyasamy, Free Radicals: Properties, Sources, Targets, and Their Implication in Various Diseases, Indian J. Clin. Biochem. 30 (2015) 11–26, https://doi.org/10.1007/s12291-014-0446-0.

[74] P. Piccinini, C. Minero, M. Vincenti, E. Pelizzetti, Photocatalytic mineralization of nitrogen-containing benzene derivatives, Catal. Today 39 (1997) 187–195, https://doi.org/10.1016/S0920-5861(97)00100-4.

[75] M.S. Priyanka, S. Mohapatra, Shifts and Trends in Analysis of Contaminants of Emerging Concern: Sulfonamides, in: M. Kumar, F. Munoz-Arriola, H. Furumai, T. Chaminda (Eds.), Resilience, Response, and Risk in Water Systems, Springer Transactions in Civil and Environmental Engineering, 2020, pp. 261–281, https://doi.org/10.1007/978-981-15-4668-6_14.

[76] Z. Qiang, C. Adams, Potentiometric determination of acid dissociation constants (pKa) for human and veterinary antibiotics, Water Res 38 (2004) 2874–2890, https://doi.org/10.1016/j.watres.2004.03.017.

[77] P.S. Rao, E. Hayon, Experimental determination of the redox potential of the superoxide radical •O2−, Biochem. Biophys. Res. Commun. 51 (1973) 468–473, https://doi.org/10.1016/0006-291X(73)91280-1.

[78] M.P. Rayaroth, C.T. Aravindakumar, N.S. Shah, G. Boczkaj, Advanced oxidation processes (AOPs) based wastewater treatment - unexpected nitration side reactions - a serious environmental issue: A review, Chem. Eng. J. 430 (2022) 133002, https://doi.org/10.1016/j.cej.2021.133002.

[79] S.G. Rizvi, S.Z. Ahammad, COVID-19 and antimicrobial resistance: A cross-study, Sci. Total Environ. 807 (2022) 150873, https://doi.org/10.1016/j.scitotenv.2021.150873.

[80] G. Sági, T. Csay, L. Szabó, G. Pátzay, E. Csonka, E. Takács, L. Wojnárovits, Sulfonamide Antibiotics in Dilute Aqueous, Solut. J. Pharm. Biomed. Anal. (2014).

[81] G. Sági, K. Szabacsi, L. Szabó, R. Homlok, K. Kovács, C. Mohácsi-Farkas, S. D. Pillai, E. Takács, L. Wojnárovits, Influence of ionizing radiation on the antimicrobial activity of the antibiotics sulfamethoxazole and trimethoprim, J. Environ. Sci. Heal. - Part A Toxic. /Hazard. Subst. Environ. Eng. 53 (2018) 687–693, https://doi.org/10.1080/10934529.2018.1439821.

[82] R.C. Scholes, Emerging investigator series: contributions of reactive nitrogen species to transformations of organic compounds in water: a critical review, Environ. Sci. Process. Impacts 24 (2022) 851–869, https://doi.org/10.1039/D2EM00102K.

[83] S.A. Snyder, P. Westerhoff, Y. Yoon, D.L. Sedlak, Pharmaceuticals, Personal Care Products, and Endocrine Disruptors in Water: Implications for the Water Industry, Environ. Eng. Sci. 20 (2003) 449–469, https://doi.org/10.1089/109287503768335931.

[84] H.S. Son, A.J. Saleh Ahammad, M.M. Rahman, K.M. Noh, J.J. Lee, Effect of nitrite and nitrate as the source of OH radical in the O3/UV process with or without benzene, Bull. Korean Chem. Soc. 32 (2011) 3039–3044, https://doi.org/10.5012/bkcs.2011.32.8.3039.

[85] M. Tahergorabi, A. Esrafili, M. Kermani, M. Gholami, M. Farzadkia, Degradation of four antibiotics from aqueous solution by ozonation: Intermediates identification and reaction pathways, Desalin. Water Treat. 139 (2019) 277–287, https://doi.org/10.5004/dwt.2019.23307.

[86] R.P. Tasho, J.Y. Cho, Veterinary antibiotics in animal waste, its distribution in soil and uptake by plants: A review, Sci. Total Environ. 563–564 (2016) 366–376, https://doi.org/10.1016/j.scitotenv.2016.04.140.

[87] A. Tekle-Röttering, E. Reisz, K.S. Jewell, H.V. Lutze, T.A. Ternes, W. Schmidt, T. C. Schmidt, Ozonation of pyridine and other N-heterocyclic aromatic compounds: Kinetics, stoichiometry, identification of products and elucidation of pathways, Water Res 102 (2016) 582–593, https://doi.org/10.1016/j.watres.2016.06.021.

[88] A. Tekle-Röttering, C. von Sonntag, E. Reisz, C. Vom Eyser, H.V. Lutze, J. Türk, S. Naumov, W. Schmidt, T.C. Schmidt, C.Vom Eyser, H.V. Lutze, J. Türk, S. Naumov, W. Schmidt, T.C. Schmidt, Ozonation of anilines: Kinetics, stoichiometry, product identification and elucidation of pathways, Water Res 98 (2016) 147–159, https://doi.org/10.1016/j.watres.2016.04.001.

[89] J. Tolls, Sorption of Veterinary Pharmaceuticals in Soils: A Review, Environ. Sci. Technol. 35 (2001) 3397–3406, https://doi.org/10.1021/es0003021.

[90] N.H. Tran, H. Chen, M. Reinhard, F. Mao, K.Y.H. Gin, Occurrence and removal of multiple classes of antibiotics and antimicrobial agents in biological wastewater treatment processes, Water Res 104 (2016) 461–472, https://doi.org/10.1016/j.watres.2016.08.040.

[91] P.G. Tratnyek, J. Hoigne, Oxidation of substituted phenols in the environment: a QSAR analysis of rate constants for reaction with singlet oxygen, Environ. Sci. Technol. 25 (1991) 1596–1604, https://doi.org/10.1021/es00021a011.

[92] S.L. Vinge, S.W. Shaheen, C.M. Sharpless, K.G. Linden, Nitrate with benefits: Optimizing radical production during UV water treatment, Environ. Sci. Water Res. Technol. 6 (2020) 1163–1175, https://doi.org/10.1039/c9ew01138b.

[93] M. Voigt, I. Bartels, A. Nickisch-Hartfiel, M. Jaeger, Photoinduced degradation of sulfonamides, kinetic, and structural characterization of transformation products and assessment of environmental toxicity, Toxicol. Environ. Chem. 99 (2017) 1304–1327, https://doi.org/10.1080/02772248.2017.1373777.

[94] C. von Sonntag, U. von Gunten, Chemistry of Ozone in Water and Wastewater Treatment: From Basic Principles to Applications, IWA Publishing,, 2012, https://doi.org/10.2166/9781780400839.

[95] L. Wang, X. Lan, W. Peng, Z. Wang, Uncertainty and misinterpretation over identification, quantification and transformation of reactive species generated in catalytic oxidation processes: A review, J. Hazard. Mater. 408 (2021) 124436, https://doi.org/10.1016/j.jhazmat.2020.124436.

[96] J.L. Weeks, G.M. Meaburn, S. Gordon, L. Weeks, G.M. Meaburn, S. Gordon, Absorption coefficients of liquid water and aqueous solutions in the far ultraviolet, Radiat. Res. 19 (1963) 559–567, https://doi.org/10.2307/3571475.

[97] L. Wojnárovits, T. Tóth, E. Takács, Critical evaluation of rate coefficients for hydroxyl radical reactions with antibiotics: A review, Crit. Rev. Environ. Sci. Technol. 48 (2018) 575–613, https://doi.org/10.1080/10643389.2018.1463066.

[98] H. Xiang, Y. Shao, N. Gao, X. Lu, W. Chu, N. An, C. Tan, X. Zheng, Y. Gao, The influence of bromide on the degradation of sulfonamides in UV/free chlorine treatment: Degradation mechanism, DBPs formation and toxicity assessment, Chem. Eng. J. 362 (2019) 692–701, https://doi.org/10.1016/j.cej.2019.01.079.

[99] P. Xie, Y. Zou, S. Jiang, J. Wang, L. Zhang, Z. Wang, S. Yue, X. Feng, Degradation of imipramine by vacuum ultraviolet (VUV) system: Influencing parameters, mechanisms, and variation of acute toxicity, Chemosphere 233 (2019) 282–291, https://doi.org/10.1016/j.chemosphere.2019.05.201.

[100] P. Xie, Y. Zou, S. Jiang, Z. Wang, J. Wang, L. Zhang, S. Yue, X. Feng, Application of vacuum-ultraviolet (VUV) to degrade β-blocker propranolol in aquatic environment: Efficiency, kinetics, pathways and acute toxicity, J. Taiwan Inst. Chem. Eng. 103 (2019) 75–84, https://doi.org/10.1016/j.jtice.2019.07.011.

[101] X. Xin, S. Sun, A. Zhou, M. Wang, Y. Song, Q. Zhao, R. Jia, Sulfadimethoxine photodegradation in UV-C/H2O2 system: Reaction kinetics, degradation pathways, and toxicity, J. Water Process Eng. 36 (2020) 101293, https://doi.org/10.1016/j.jwpe.2020.101293.

[102] L. Yang, Z. Zhang, Degradation of six typical pesticides in water by VUV/UV/chlorine process: Evaluation of the synergistic effect, Water Res 161 (2019) 439–447, https://doi.org/10.1016/j.watres.2019.06.021.

[103] S.Y. Yang, Y. yuan Chen, J. guo Zheng, Y. jie Cui, Enhanced photocatalytic activity of TiO2 by surface fluorination in degradation of organic cationic compound, J. Environ. Sci. 19 (2007) 86–89, https://doi.org/10.1016/S1001-0742(07)60014-X.

[104] X. Yang, J. Peng, B. Chen, W. Guo, Y. Liang, W. Liu, L. Liu, Effects of ozone and ozone/peroxide pretreatments on disinfection byproduct formation during subsequent chlorination and chloramination, J. Hazard. Mater. 239–240 (2012) 348–354, https://doi.org/10.1016/j.jhazmat.2012.09.006.

[105] Z. Yi, J. Wang, Q. Tang, T. Jiang, Photolysis of sulfamethazine using UV irradiation in an aqueous medium, RSC Adv. 8 (2018) 1427–1435, https://doi.org/10.1039/c7ra09564c.

[106] H. Yu, P. Ge, J. Chen, H. Xie, Y. Luo, The degradation mechanism of sulfamethoxazole under ozonation: a DFT study, Environ. Sci. Process. Impacts 19 (2017) 379–387, https://doi.org/10.1039/C6EM00698A.

[107] S.M. Zainab, M. Junaid, N. Xu, R.N. Malik, Antibiotics and antibiotic resistant genes (ARGs) in groundwater: A global review on dissemination, sources, interactions, environmental and human health risks, Water Res 187 (2020) 116455, https://doi.org/10.1016/j.watres.2020.116455.

[108] R. Zhang, Y. Yang, C.-H.H. Huang, L. Zhao, P. Sun, Kinetics and modeling of sulfonamide antibiotic degradation in wastewater and human urine by UV/H 2 O 2 and UV/PDS, Water Res 103 (2016) 283–292, https://doi.org/10.1016/j.watres.2016.07.037.

[109] G. Zhu, Q. Sun, C. Wang, Z. Yang, Q. Xue, Removal of sulfamethoxazole, sulfathiazole and sulfamethazine in their mixed solution by UV/H2O2 process, Int. J. Environ. Res. Public Health 16 (2019), https://doi.org/10.3390/ijerph16101797.